Elettra Sincrotrone Trieste

Cathode Lens Microscopy
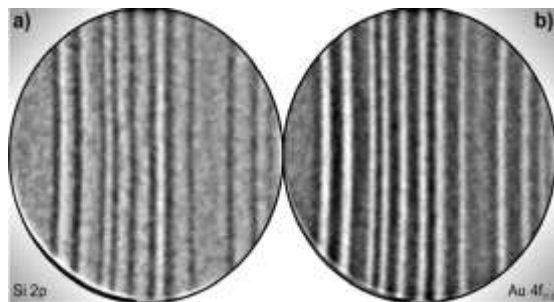# LEEM, XPEEM and Applications
part1: Methods

Andrea Locatelli

Andrea.locatelli@elettra.eu

# Why do we need spectromicroscopy?

- To combine SPECTROSCOPY and MICROSCOPY to characterise the structural, chemical and magnetic properties of surfaces, interfaces and thin films

- Applications in diverse fields such as surface science, catalysis, material science, magnetism but also geology, soil sciences, biology and medicine.
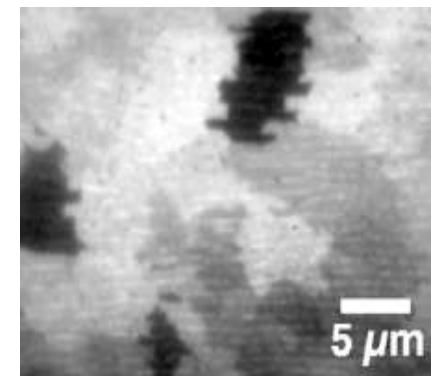
Surface Science

Magnetism

Biology

Co

Interface

NiO

5 μm

DOI: 10.1103/PhysRevLett.86.5088
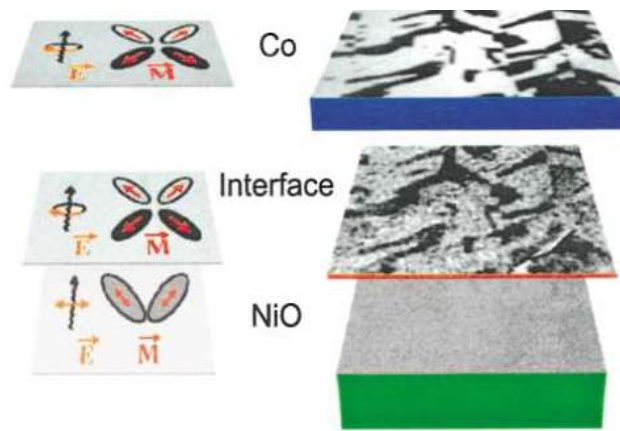
DOI: 10.1103/PhysRevLett.87.247201

PRL **98**, 268102 (2007)

Outline

- **Synchrotron radiation methods**

- **X-ray spectro-microscopy:**

  - **Cathode lens microscopy instrumentation**

  - **XPEEM/LEEM**

- **Applications**

  - **Chemical imaging of micro- structured materials**

    Graphene research.

  - **Biology**

  - **Magnetic imaging**

  - **Time-resolved**

Why does microscopy need SR?

- **High intensity** of SR makes measurements faster
- **Tuneability** – very broad and continuous spectral range from IR to hard X-Rays
- Narrow angular collimation
- Coherence!
- **High degree of polarization**
- **Pulsed time structure** of SR – This adds time resolution to photoelectron spectroscopy!
- Quantitative control on SR parameters allows spectroscopy:
  - Absorption Spectroscopy (XAS and variants)
  - Photoemission Spectroscopies (XPS, UPS, ARPES, ARUPS)

$$J = f(h\nu, \varepsilon, \Theta, \Phi; E_{kin}^{e}, \sigma, \theta_e, \varphi_e)$$

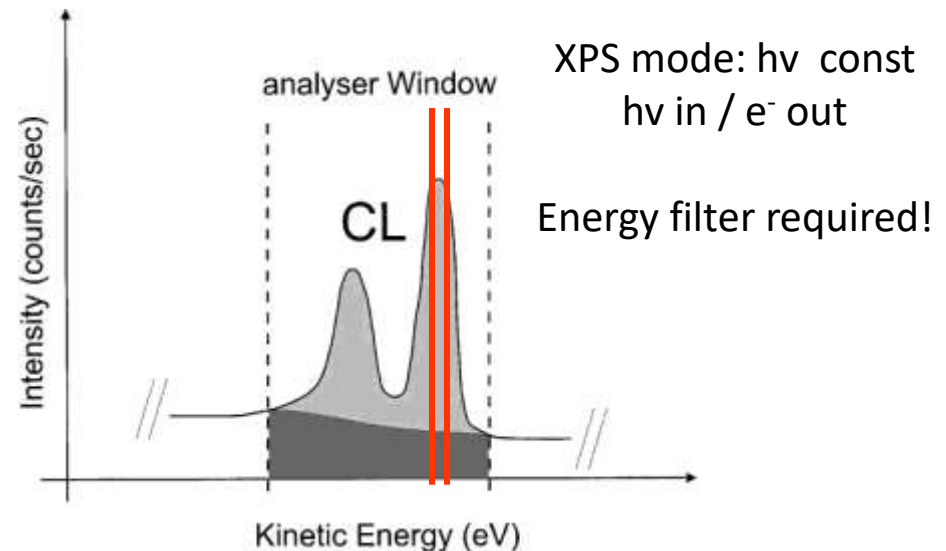# X-ray Photoelectron Spectroscopy

The absorption of a photon ionizes the system, exciting one of the electrons into a free state in the continuum. The transition probability from the initial state to the final is proportional to:

$$\tau_{ik} \propto 4\pi^2 \alpha \hbar \omega \left| \langle \psi_i | \hat{e} \cdot \hat{r} | e^{jkr} \rangle \right|^2 \delta(E_i + \hbar\omega - \frac{\hbar^2 k^2}{2m})$$

We measure the energy distribution of the photoelectrons emitted from the specimen.

$$E_k = h\nu - E_B - \Phi$$

E_B is the binding energy of the initial state. E_B is a unique fingerprint that allows determining the composition and chemical state of the specimen surface. This is the founding principle of ESCA and XPS (K. Siegbahn's Nobel prize).


XPS mode: hv const
hv in / e⁻ out

Energy filter required!

Main features: Elemental and chemical sensitivity (surface core level shifts), sensitivity to the electronic structure, sensitivity to local structure (micro-XPD), highest surface sensitivity

X-ray absorption spectroscopy basics

$$\mu = 4\pi^2 \alpha \hbar \omega \sum_k \left| \langle \psi_k | \hat{\varepsilon} \cdot \hat{r} | \psi_c \rangle \right|^2 \delta(e_k - e_c - \hbar\omega)$$

energy dependent absorption of x-rays! Resonances arise from transitions from core levels into unoccupied valence states via excitation processes occurring during the filling of the core hole.
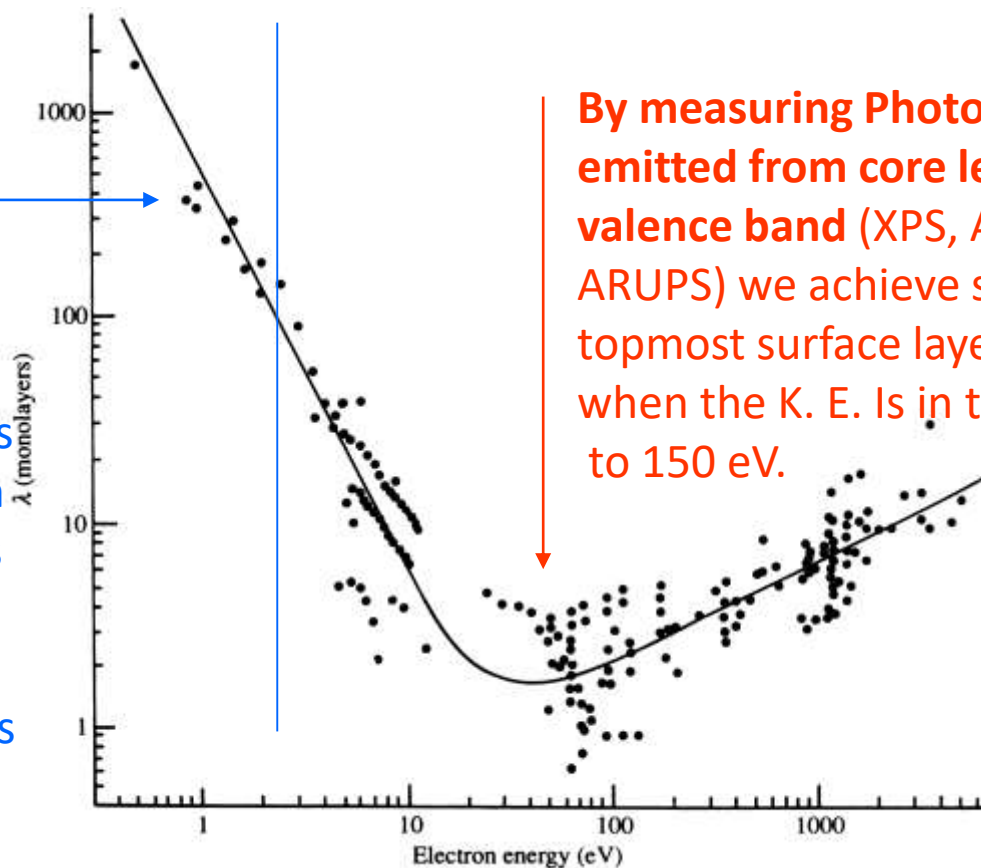

https://www-ssrl.slac.stanford.edu/stohr/xmcd.htm
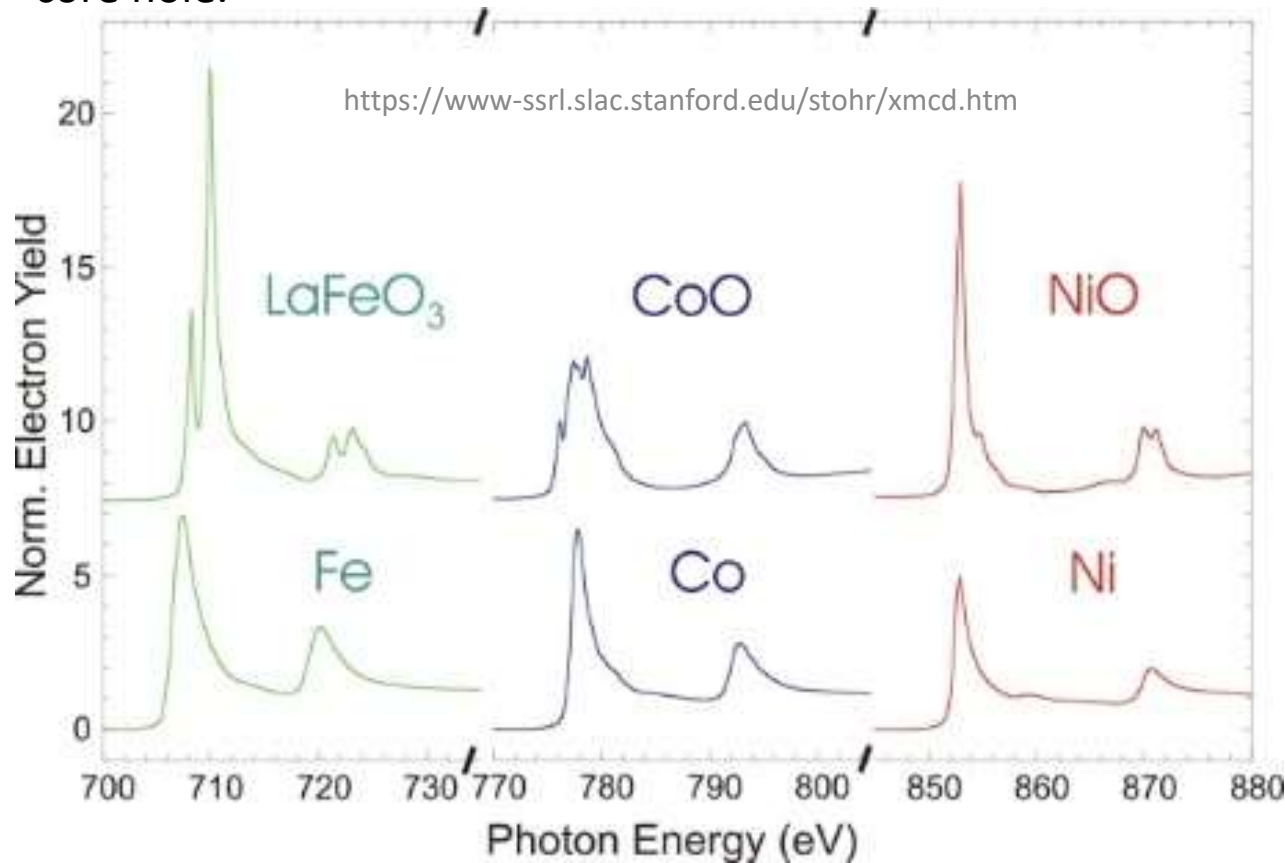
✓ Elemental sensitivity.
✓ Chemical sensitivity
✓ Electronic charge
   ✓ valence state,
   ✓ bond orientation

We measure:
- Absorption through the material
- Secondary electron yield
- Escape depth of low energy electrons gives access to buried layers

Energy dependent electron probing depth

Inelastic mean free path ("universal curve")

By measuring secondary Electrons we probe thin films and buried interfaces to a maximum depth of several nm. This is the case of X-ray absorption spectro-scopy and its variants (NEXAFS, XMCD, XMLD).

By measuring Photoelectrons emitted from core levels or the valence band (XPS, ARPES, UPS, ARUPS) we achieve sensitivity to the topmost surface layers, especially when the K. E. Is in the range 50 to 150 eV.

SR tuneability & photoionization cross sections

Choosing the best photon energy for the experiment is of crucial importance to maximize surface / elemental sensitivity as well as obtaining favourable acquisition times
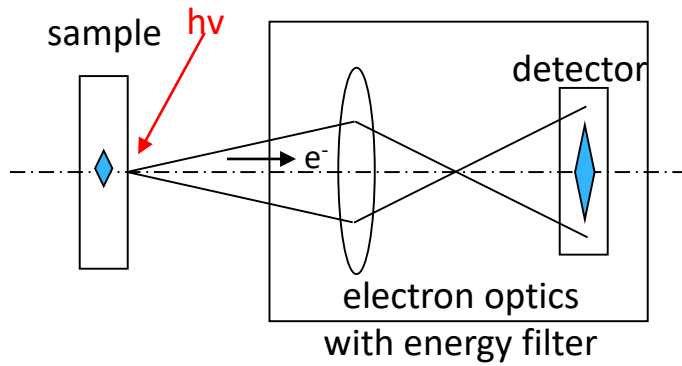
Graphene / Ru(0001)

Yeh and Lindau, *Atomic Data and Nuclear Data Tables* **32**, I-I 55 (1985)
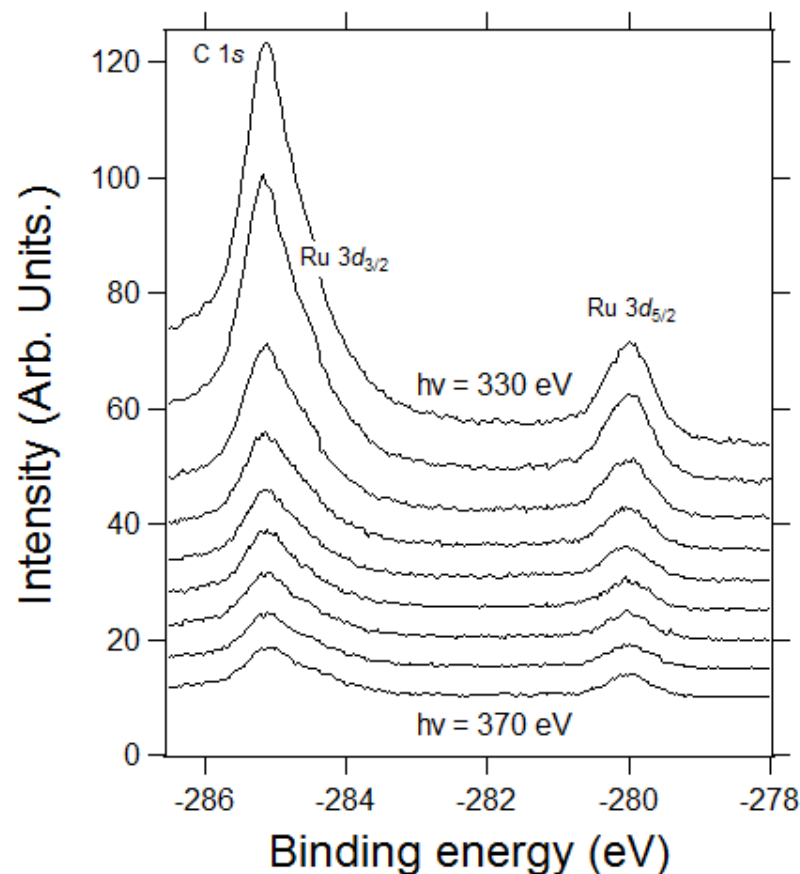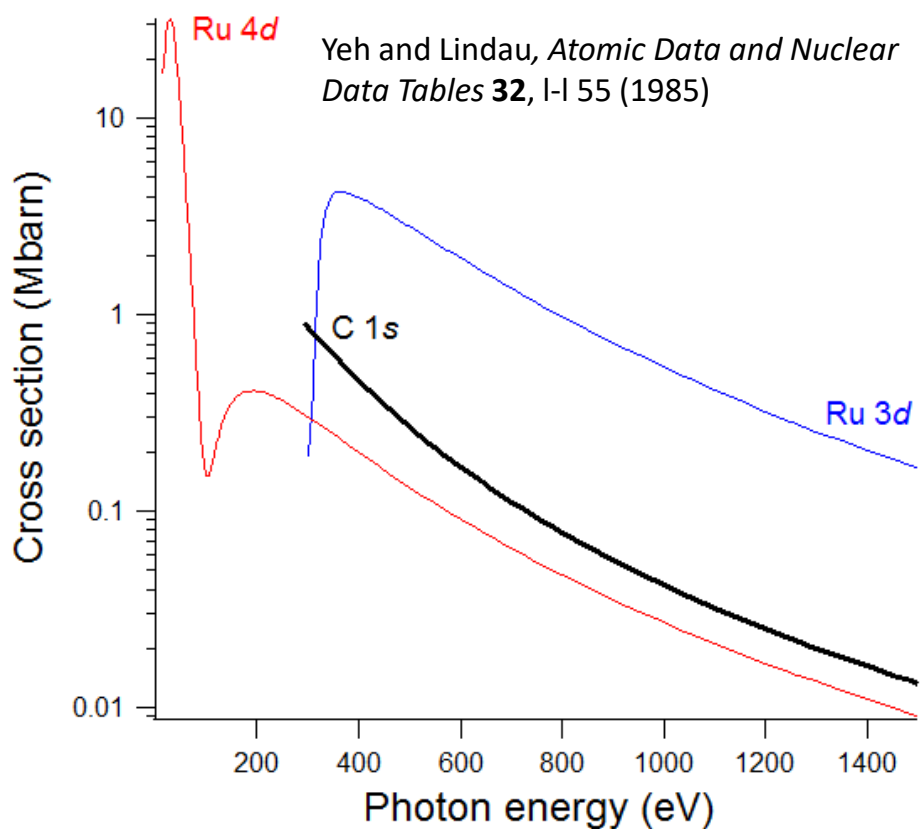
The two main approaches of x-ray microscopy

X-ray photoemission electron microscopy (XPEEM)

sample   hv   detector   e⁻   electron optics with energy filter

Scanning photoemission electron microscopy (SPEM)

x-ray optics   electron analyzer   sample scanning stage   x-ray detector   hv

- Direct imaging, parallel detection
- Lateral resolution determined by electron optics: aberration correction nowadays possible with resolution < 2nm
- Combination with LEEM/LEED
- Intermediate spectroscopic ability
- $P_{max} < 5 \cdot 10^{-5}$ mbar
- Flat surfaces
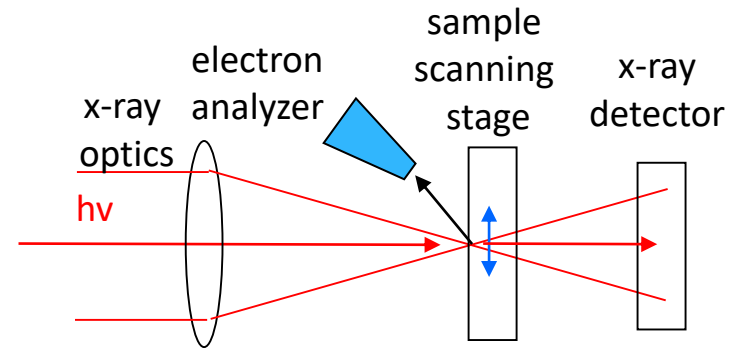
- Scanning: sequantial indirect imaging
- Lateral resolution determined by X-ray (diffractive) optics: 20-30 nm.
- Combination with TXM
- Excellent spectroscopic ability
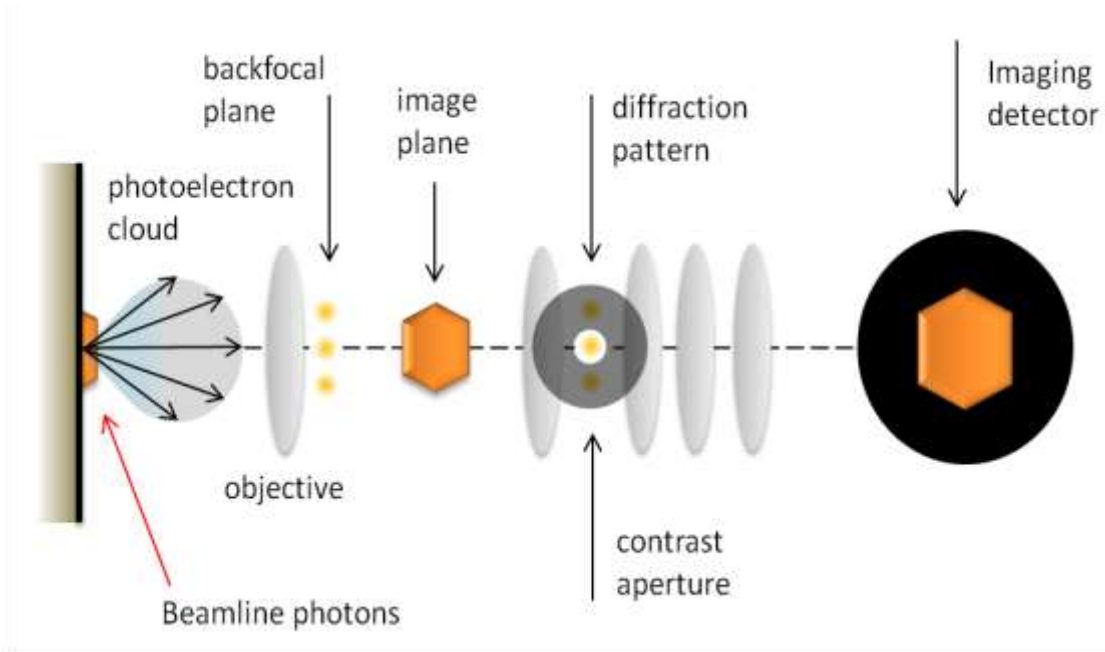- High pressure variants do exisits
- Rough surfaces

Microscopies and chemical sensitivity
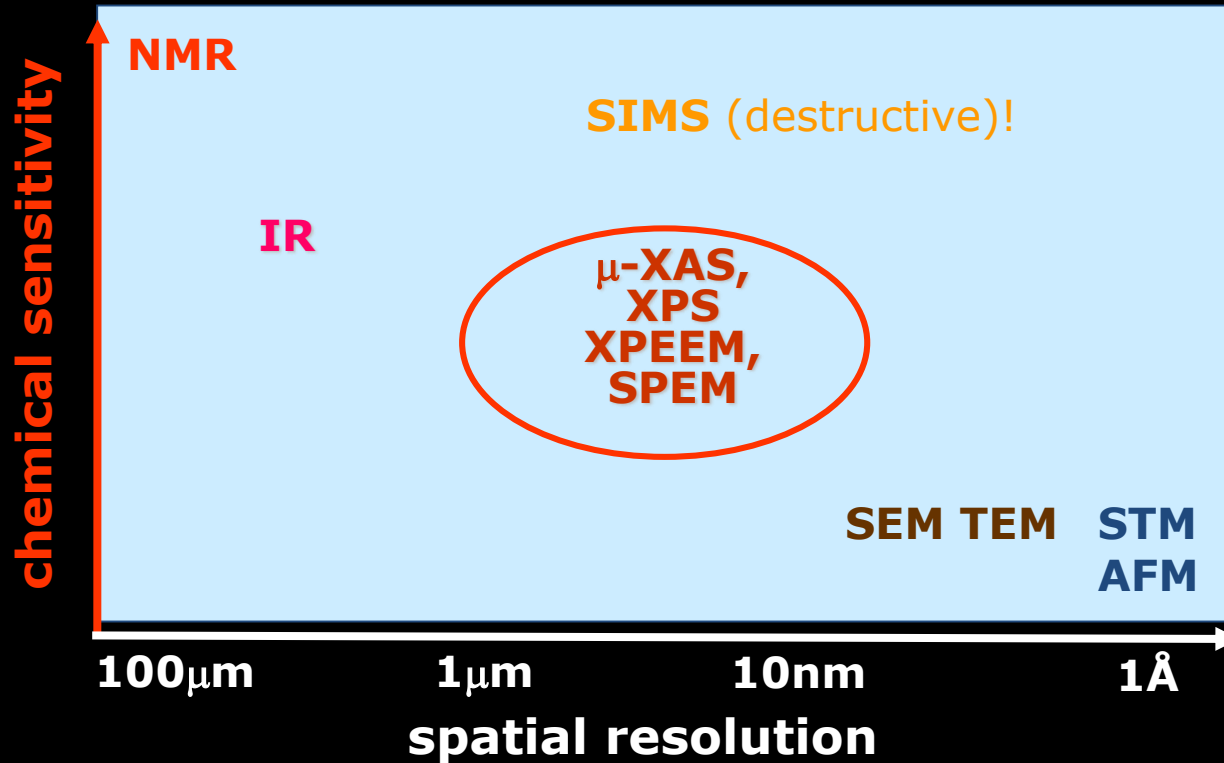
Cathode lens microscopy methods

PEEM, LEEM, SPELEEM, AC-PEEM/LEEM

PEEM basics

- Direct imaging, parallel detection
- Lateral resolution determined by electron optics: with AC, few nm possible
- Elemental sensitivity (XAS)
- Spectroscopic ability (energy filter)
- $P_{max} < 5 \cdot 10^{-5}$ mbar

PEEM is a full-field technique. The microscope images a restricted portion of the specimen area illuminated by x-ray beam. Photoemitted electrons are collected at the same time by the optics setup, which produces a magnified image of the surface. The key element of the microscope is the objective lens, also known as cathode or immersion lens, of which the sample is part

Cathode lens operation principle

1. In emission microscopy θ (emission angle) is large. Electron lenses can accept only small θ because of large chromatic and spherical aberrations

2. Solution of problem: accelerate electrons to high energy before lens $\rightarrow$ Immersion objective lens or cathode lens

$n \sin\theta = const$

$n \sim \sqrt{E}$

$\theta \rightarrow \alpha$

$\sin\alpha / \sin\alpha_0 = \sqrt{E_0/E}$

Example for E = 20000 eV:

	E_0	2 eV	200 eV
α for $\alpha_0 = 45°$		0.4°	4.5°

3. The aberrations of the objective lens and the contrast aperture size determine the lateral resolution

$$d = \sqrt{d_{SP}^2 + d_{CH}^2 + d_D^2}$$

$$d_D = 0.6\, \lambda / r_A$$
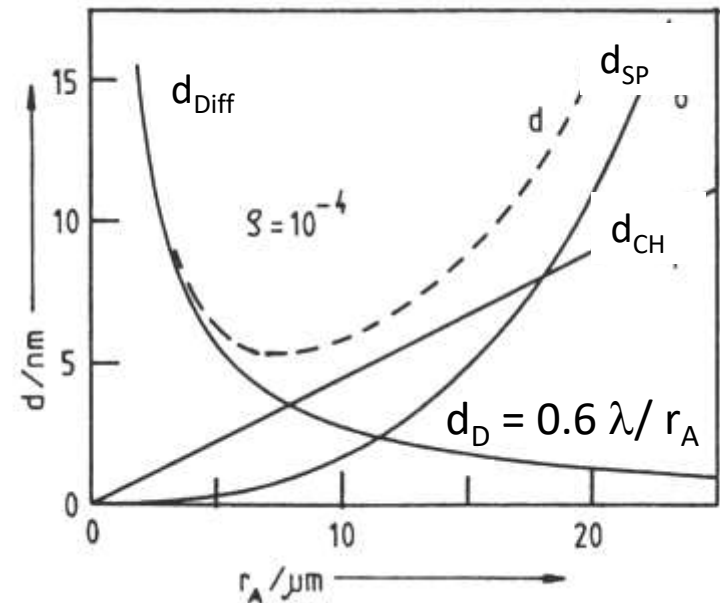
The different types of PEEM measurements

PEEM	Probe	Measurement
threshold microscopy	Hg lamp	photoelectrons
Laterally resolved XPS, micro-spectroscopy	X-ray	core levels or VB ph.el.
Laterally resolved UPS, microprobe ARUPS /ARPES	X-rays, He lamp	VB photoelectrons
Auger Spectroscopy	X-ray, or electrons	secondary electrons
XAS-PEEM (XMC/LD-PEEM)	X rays	secondary electrons

Require energy filter

Low energy electron microscopy (LEEM)
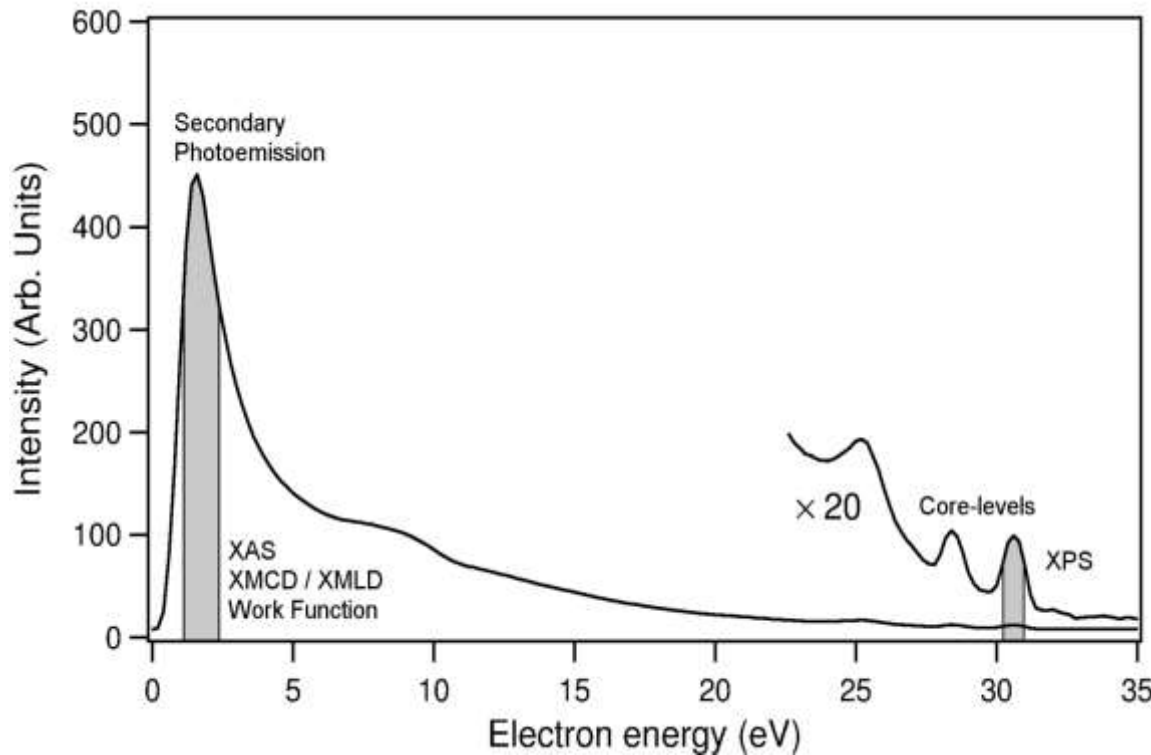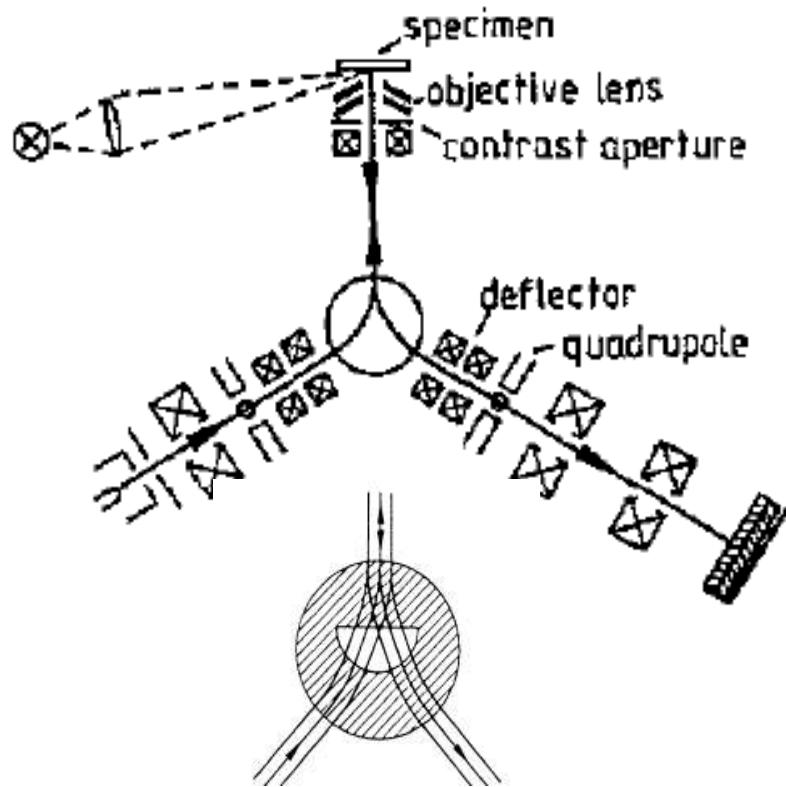
Backscattering cross section
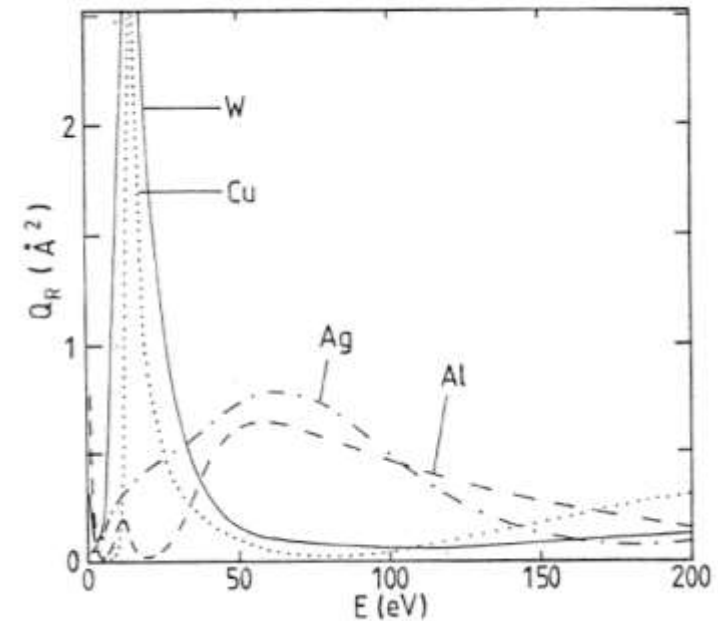
E. Bauer, Rep. Prog. Phys. 57 (1994) 895-938.

- LEEM probes surfaces with low energy electrons, using the elastically backscattered beam for imaging.
- Direct imaging and diffraction imaging modes

- High structure sensitivity
- High surface sensitivity
- Video rate: reconstructions, growth, step dynamics, self-organization

Image contrast in LEEM

Different contrast mechanisms are available for strucutre characterization

SURFACE STRUCTURE

dark-field LEEM   bright-field LEEM 8 eV

)

FILM THICKNESS

Co/W(110)

STEP MORPHOLOGY

Mo(110)

1 µm

diffraction contrast

sample

objective

[h,j]

[0,0]

contrast aperture
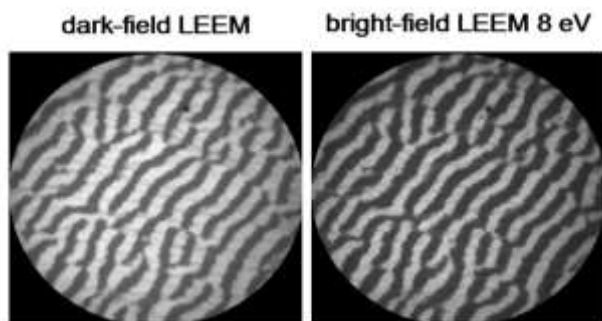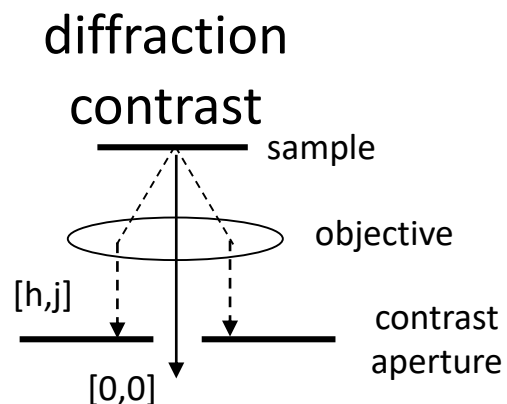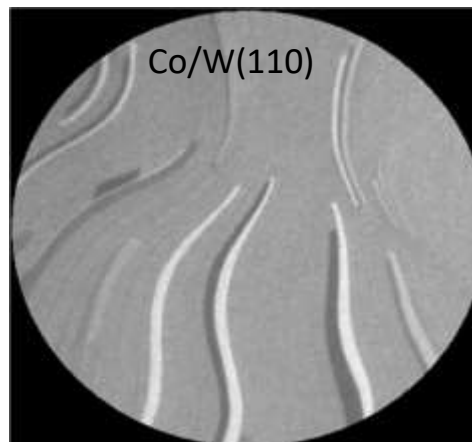
quantum size contrast

d
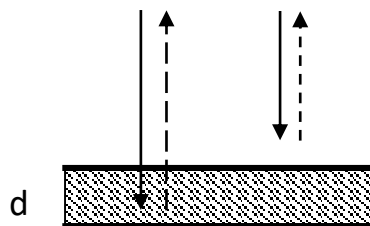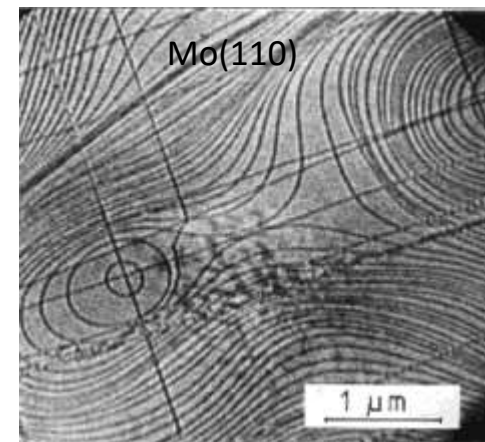
geometric phase contrast

SPELEEM = LEEM + PEEM

LEEM - Structure sensitivity

energy filter

separator

e-gun

sample

XPEEM - Chemical and electronic structure sensitivity
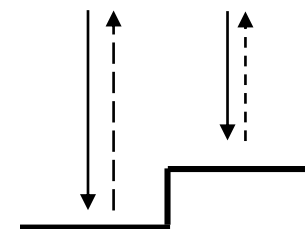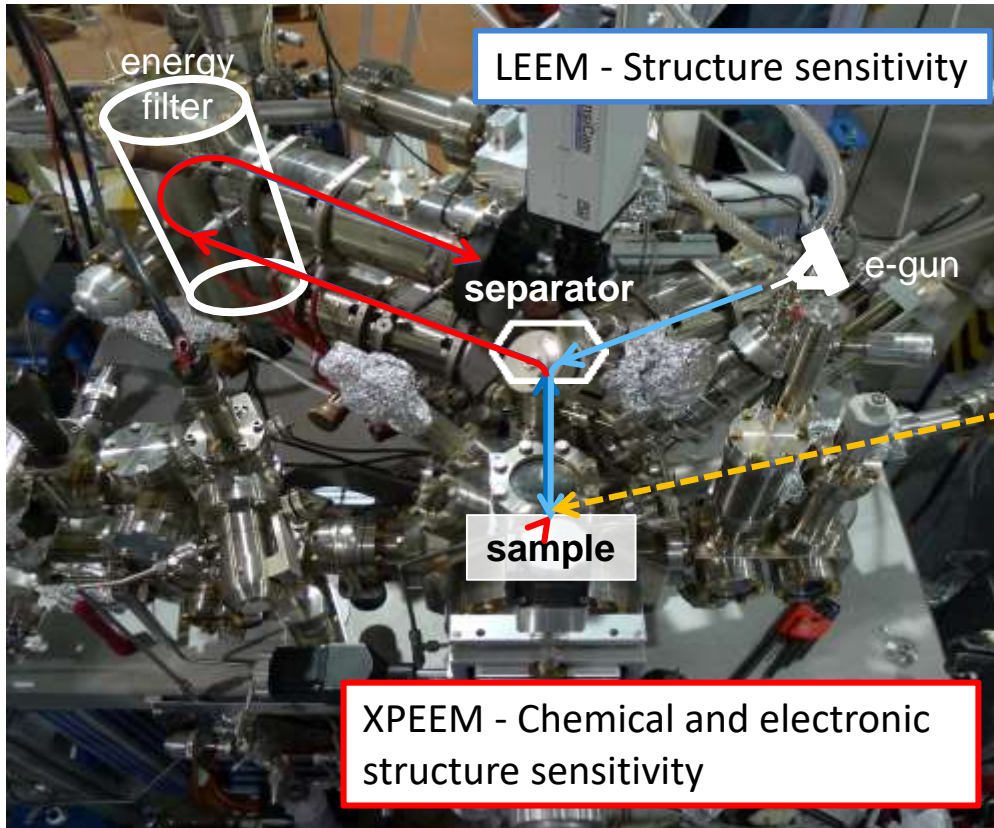
The Nanospectroscopy beamline@Elettra

Flux on the sample: 10^{13}ph/sec (microspot) intermediate energy resolution.
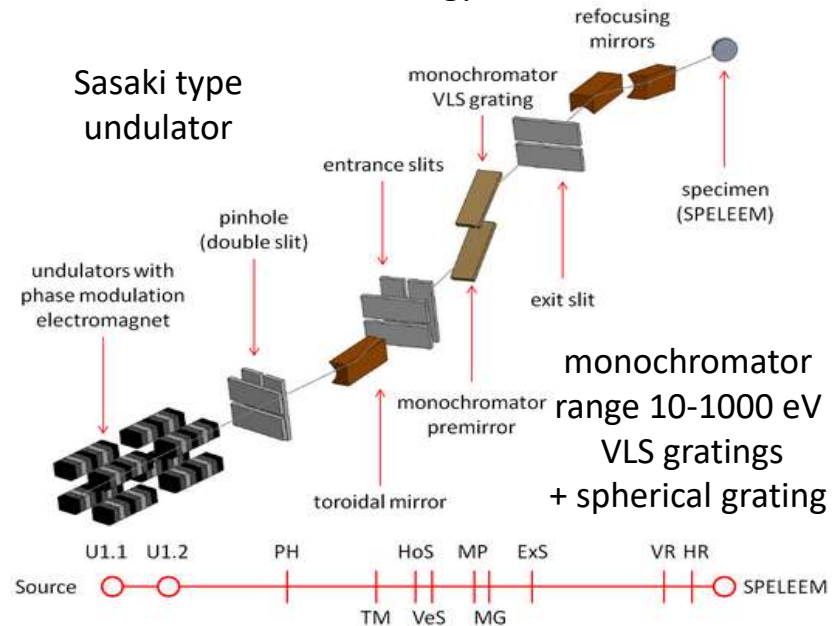
Sasaki type undulator

refocusing mirrors

monochromator VLS grating

entrance slits

pinhole (double slit)

undulators with phase modulation electromagnet

monochromator premirror

toroidal mirror

specimen (SPELEEM)

exit slit

monochromator range 10-1000 eV VLS gratings + spherical grating

U1.1 U1.2   PH   HoS MP ExS   VR HR

Source O   O | | | | | | O SPELEEM

TM   VeS   MG

Applications:
characterization of materials at microscopic level, magnetic imaging of micro-structures Imaging of dynamical processes

A. Locatelli, L. Aballe, T.O. Menteş, M. Kiskinova, E. Bauer, Surf. Interface Anal. 38, 1554-1557 (2006)

T. O. Menteş, G. Zamborlini, A. Sala, A. Locatelli; Beilstein J. Nanotechnol. 5, 1873–1886 (2014)

SPELEEM many methods analysis
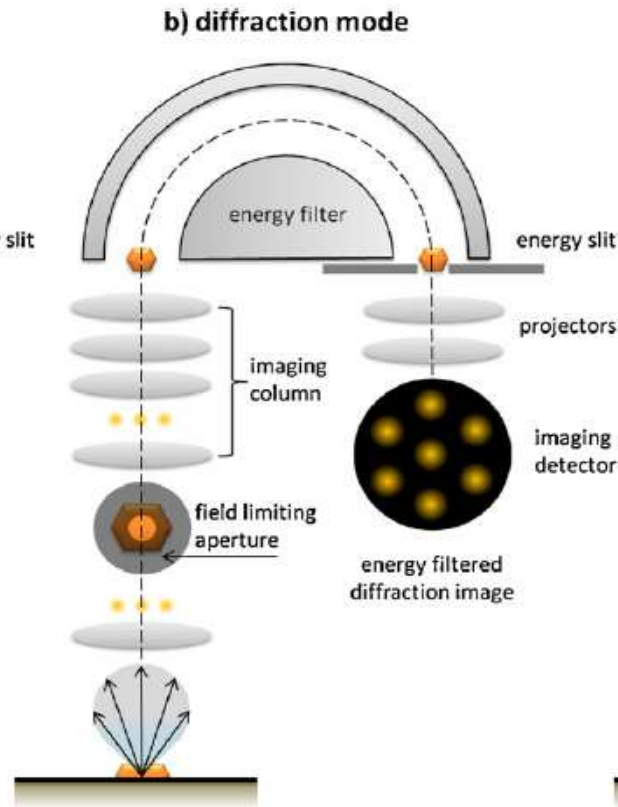
Spectroscopic imaging
XAS-PEEM / XPEEM / LEEM

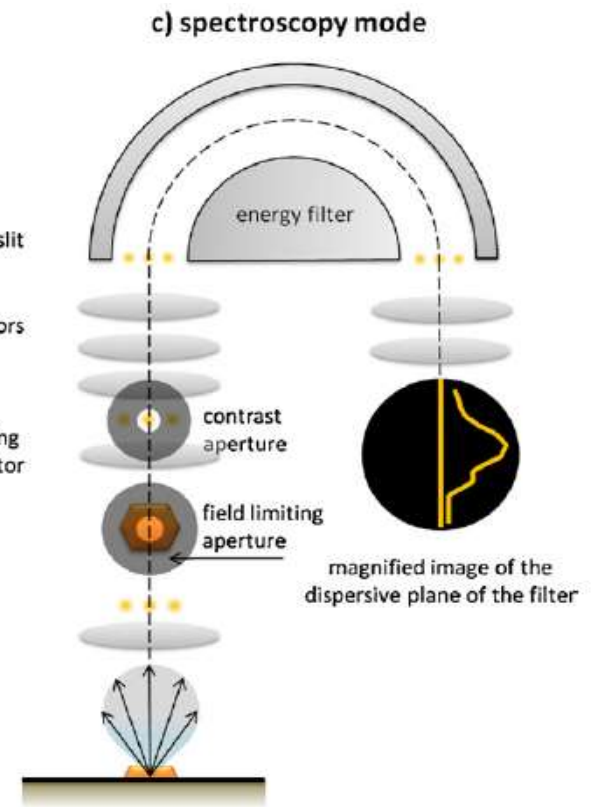microprobe-diffraction
ARPES / LEED

microprobe-spectroscopy
XPS

a) imaging mode

b) diffraction mode

c) spectroscopy mode

spatial resolution
LEEM : 10 nm
XPEEM : 25 nm

energy resolution
XPEEM : 0.3 eV

Limited: to 2 microns in dia.
angular resolution
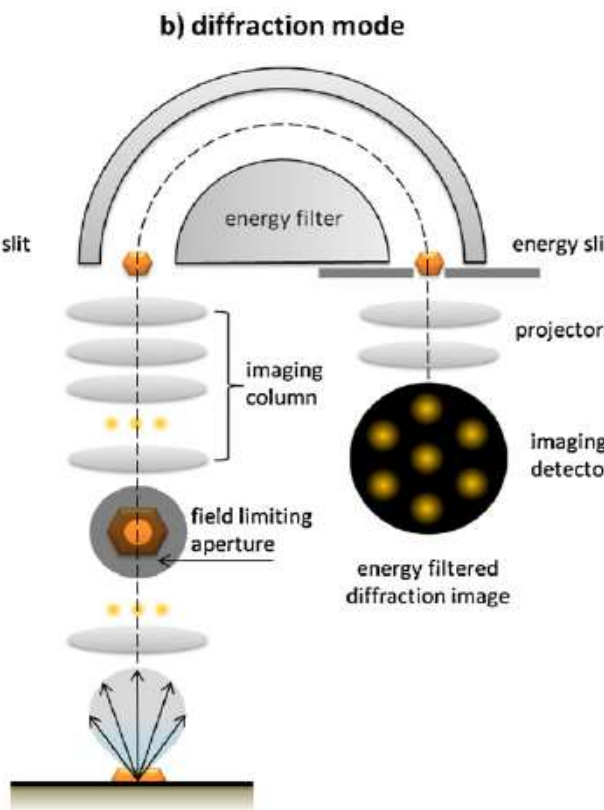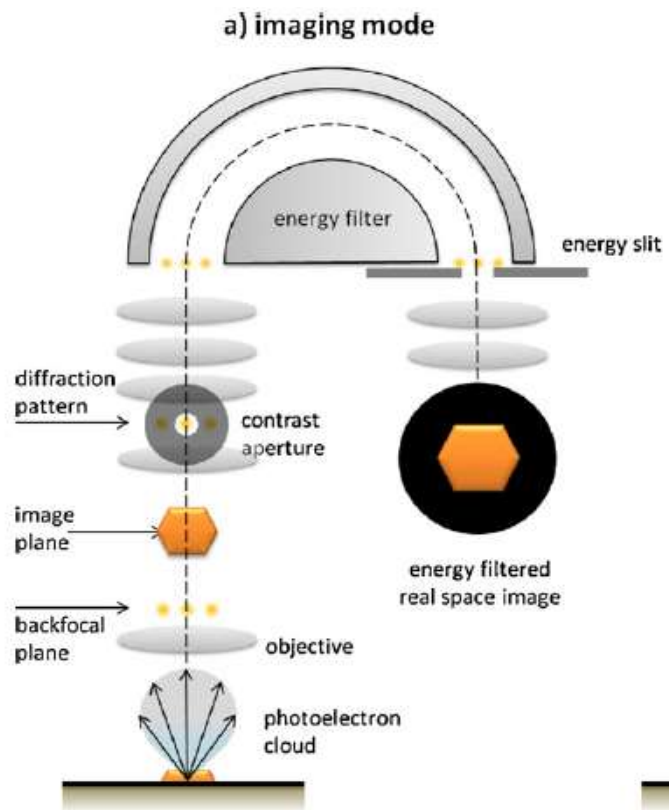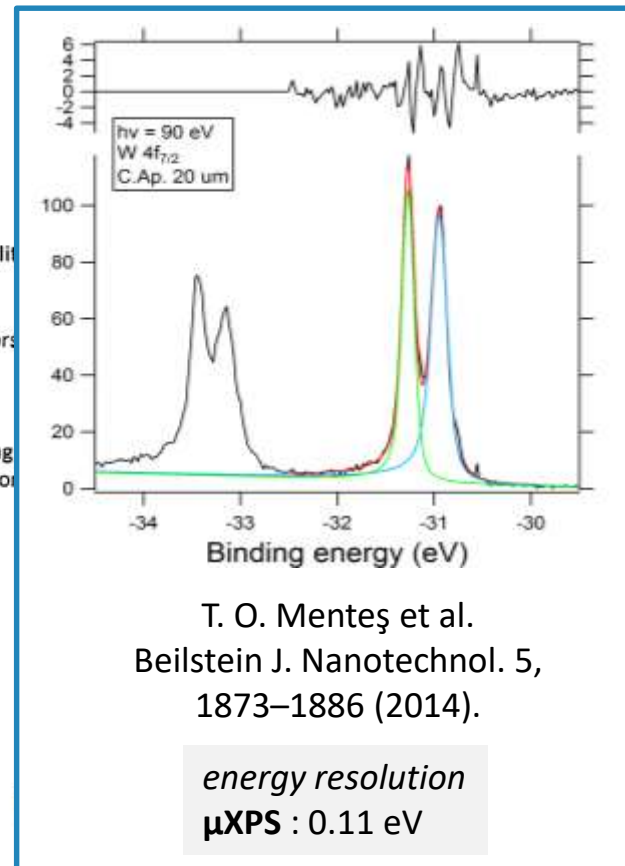**transfer width**: 0.01 Å^{-1}

SPELEEM many methods analysis

Spectroscopic imaging
XAS-PEEM / XPEEM / LEEM

microprobe-diffraction
ARPES / LEED

microprobe-spectroscopy
XPS

a) imaging mode

b) diffraction mode

T. O. Menteş et al.
Beilstein J. Nanotechnol. 5,
1873–1886 (2014).

energy resolution
μXPS : 0.11 eV

spatial resolution
LEEM : 10 nm
XPEEM : 25 nm

energy resolution
XPEEM : 0.3 eV

Limited: to 2 microns in dia.
angular resolution
transfer width: 0.01 Å^{-1}

SPELEEM summary

Performance: <u>lateral resolution</u> in imaging: 10nm (LEEM)
30 nm (XPEEM)

<u>energy resolution</u>: 0.3 eV (0.1 eV muXPS)

Key feature: <u>multi-method</u> instrument to the study of surfaces and interfaces offering *imaging* and *diffraction* techniques.

Probe: *low energy e-* (0-500 eV) ⟷ structure sensitivity
soft X-rays (50-1000 eV) ⟷ chemical state, magnetic state, electronic struct.

Applications: *characterization* of materials at microscopic level
magnetic imaging of microstrucutres
dynamical processes

I will focus on

Surfaces, interfaces and thin films

Part2: XPEEM Applications:
Imaging the Chemical and Electronic Structure

Andrea Locatelli

Andrea.locatelli@elettra.eu

Thickness dependent reactivity in Mg
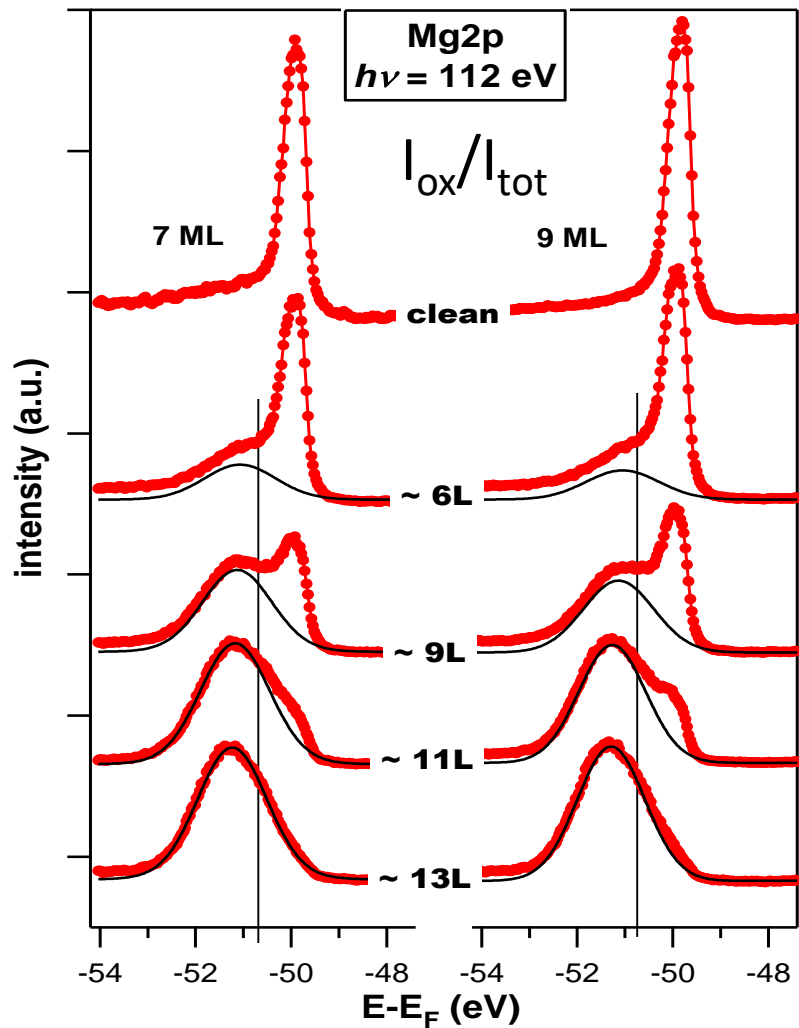
Oxide component reveals chemistry!

L. Aballe *et al.*, Phys. Rev. Lett. **93**, 196103 (2004)

Oxidation of Mg film and quantum well states
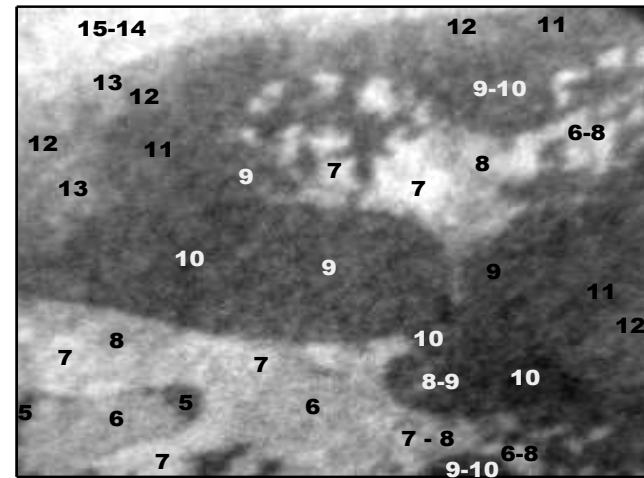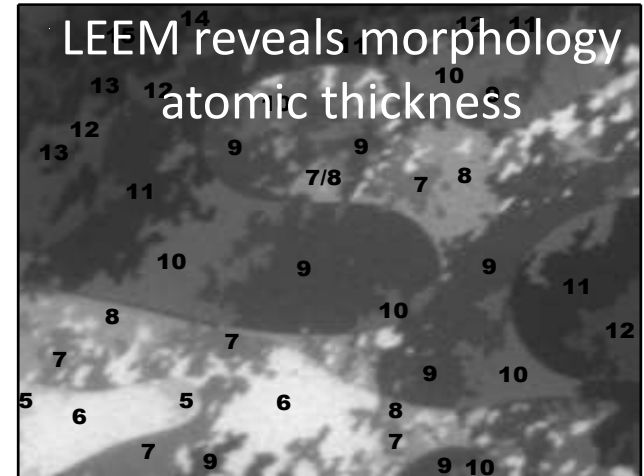
FACTS

✓ Strong variations in the oxidation extent are correleted to thickness and to the density of states at E_F

✓ XPEEM is a powerful technique for correlating chemistry and electronic structure information

SIGNIFICANCE OF THE EXPERIMENTS

✓ Control on film thickness enables modifying the molecule-surface interaction

✓ Theoretical explanation: Decay length of QWS into vacuum is critical: it reproduces peak of reactivity in experimental data. See Binggeli and M. Altarelli, Phys.Rev.Lett. 96, 036805 (2005)
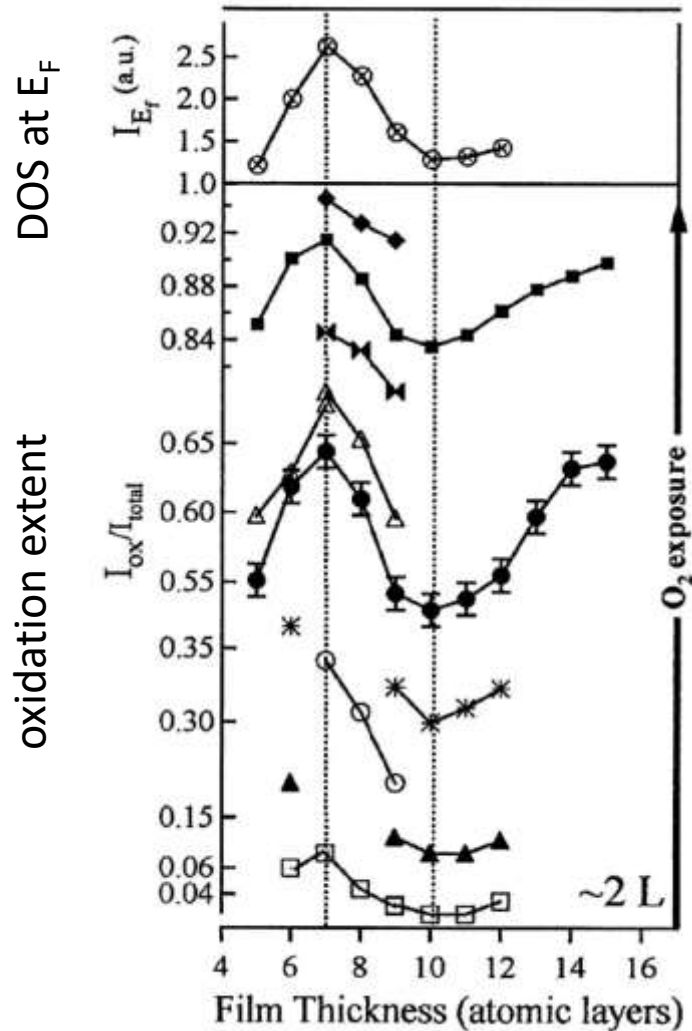
L. Aballe *et al.*, Phys. Rev. Lett. 93, 196103 (2004)

The complexity of the metal-graphene interface

adsorption, intercalation,

Irradiation, functionalization, implantation

corrugations

strain

Vacancies & defects

edges

Substrate

Buffer layer
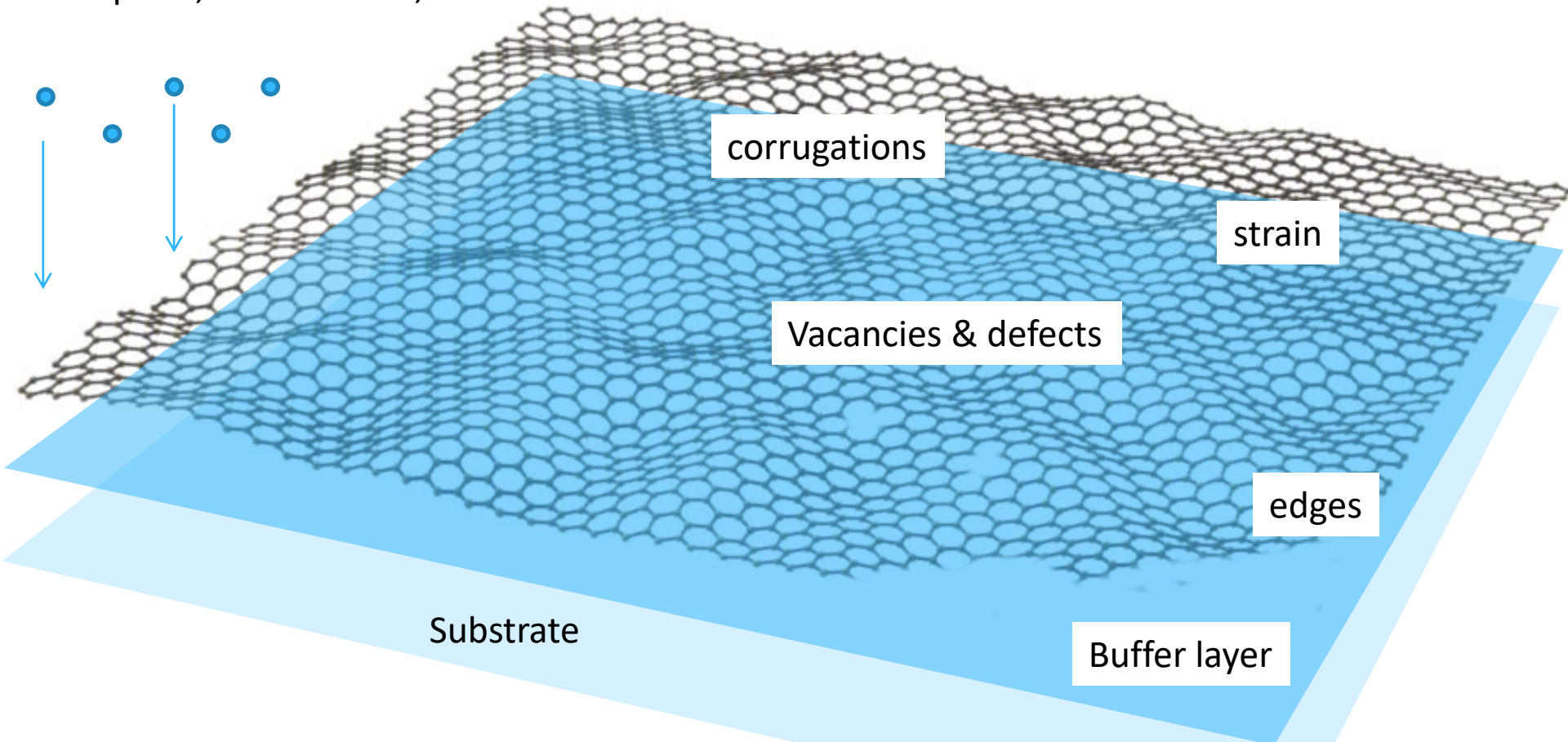
- Understand and control the fundamental interactions occurring at the interface
- verify the properties (crystal quality, stoichiometry, electronic structure) at the mesoscale!

XPEEM studies of graphene

- Effect of substrate' symmetry
  - The complex structure of g/Ir(100)
- Buffers
  - Au Intercalation
  - Carbides in graphene on Ni(111)
- Irradiation/implantation
  - Low energy N+ ion irradiation of g/Ir(111)
  - [Irradiation with noble gases of g/Ir(100)]

graphene growth on Ir(001)

Growth 600°C < T < 670°Cb P_{C2H4} =2·10^{-8} mbar   growth at T > 800°C

microprobe-LEED: graphene

BF-LEEM   DF-LEEM

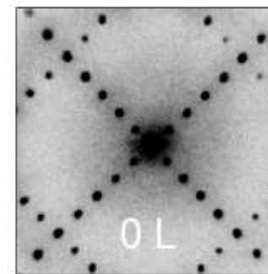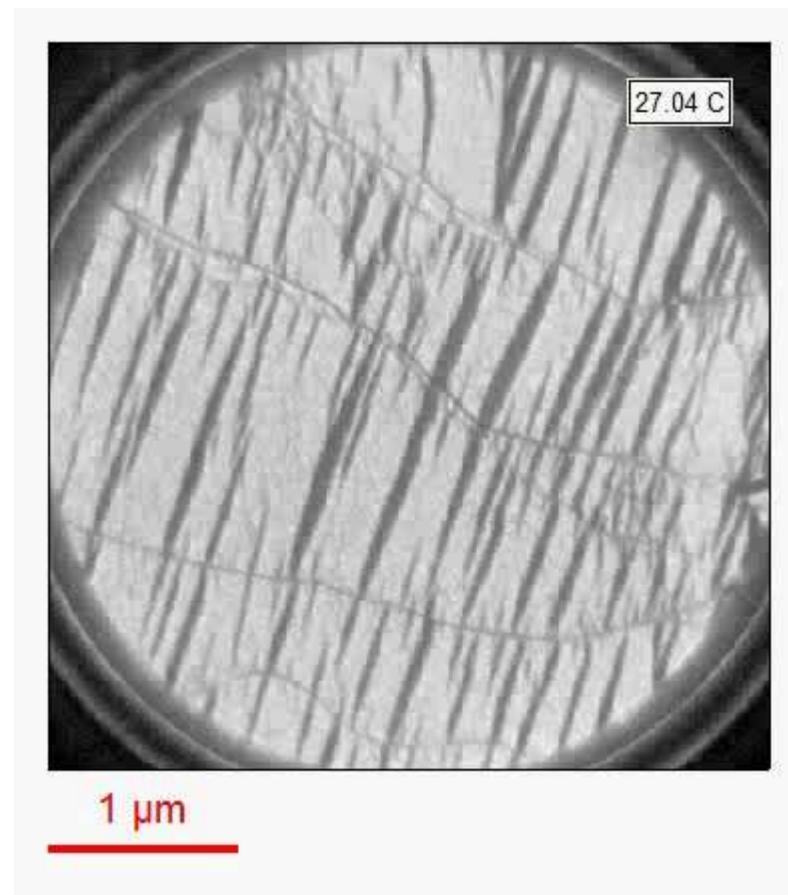2 μm   A (centre)   A (side)   B

0 L   4.3 L   8.7 L

A. Locatelli, G. Zamborlini, T.O. Menteş; Carbon 74, 237–248 (2014);
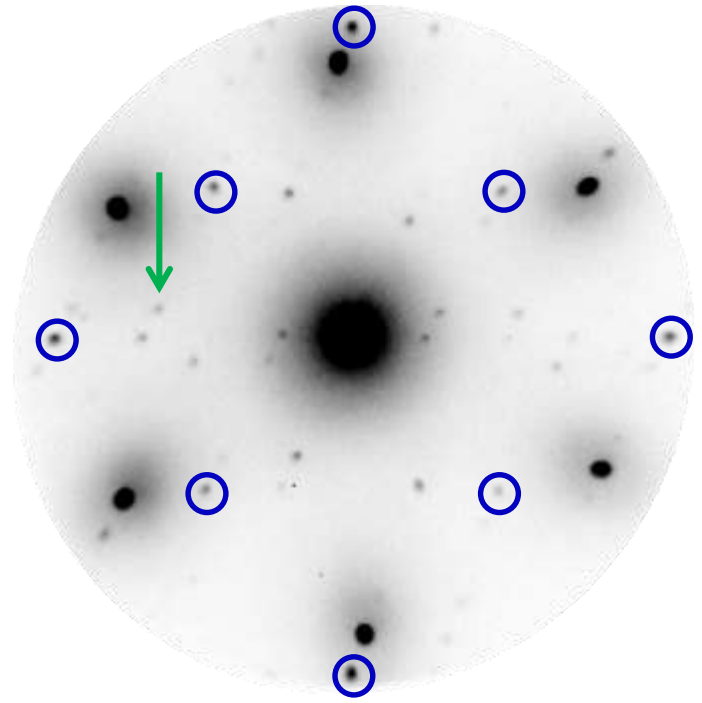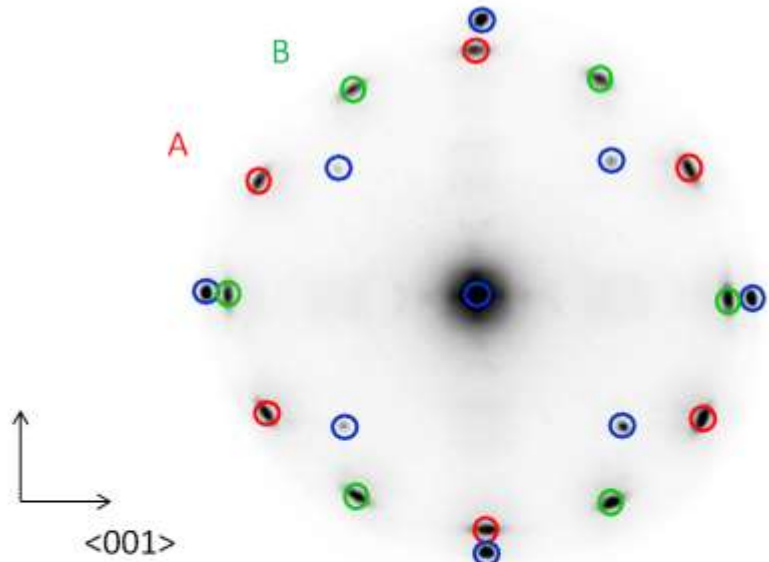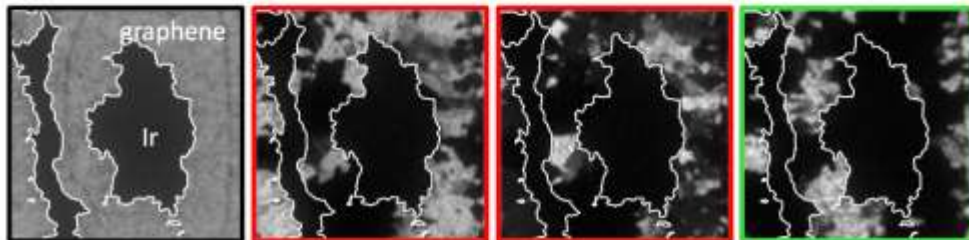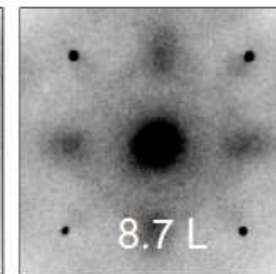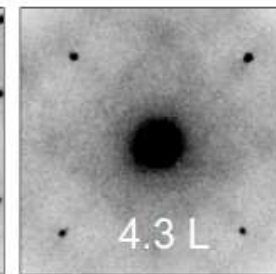
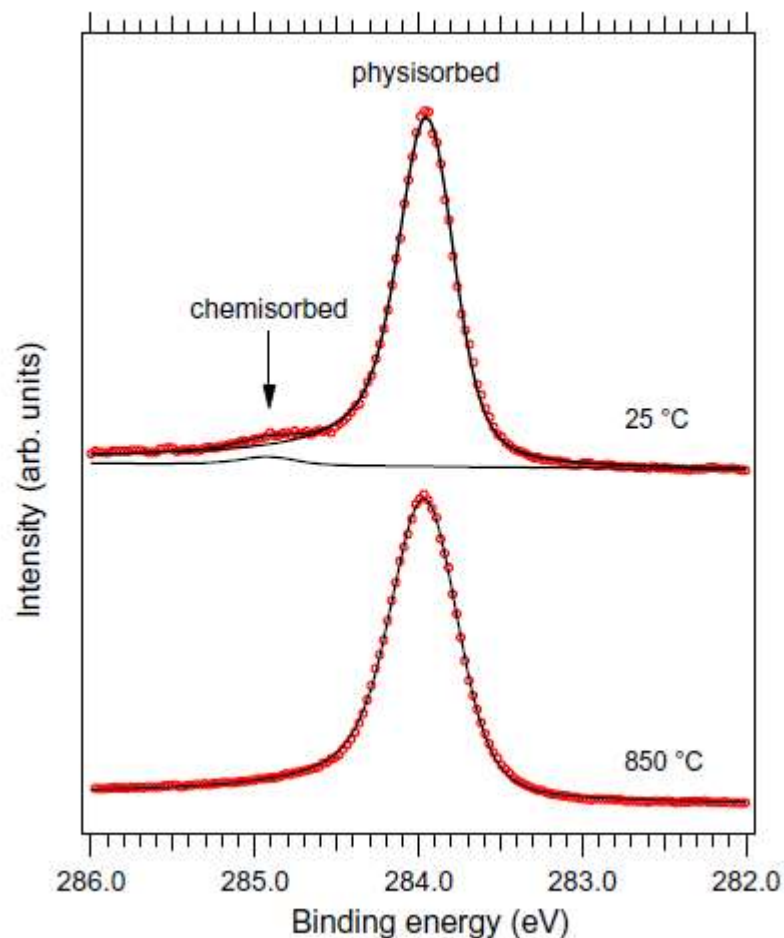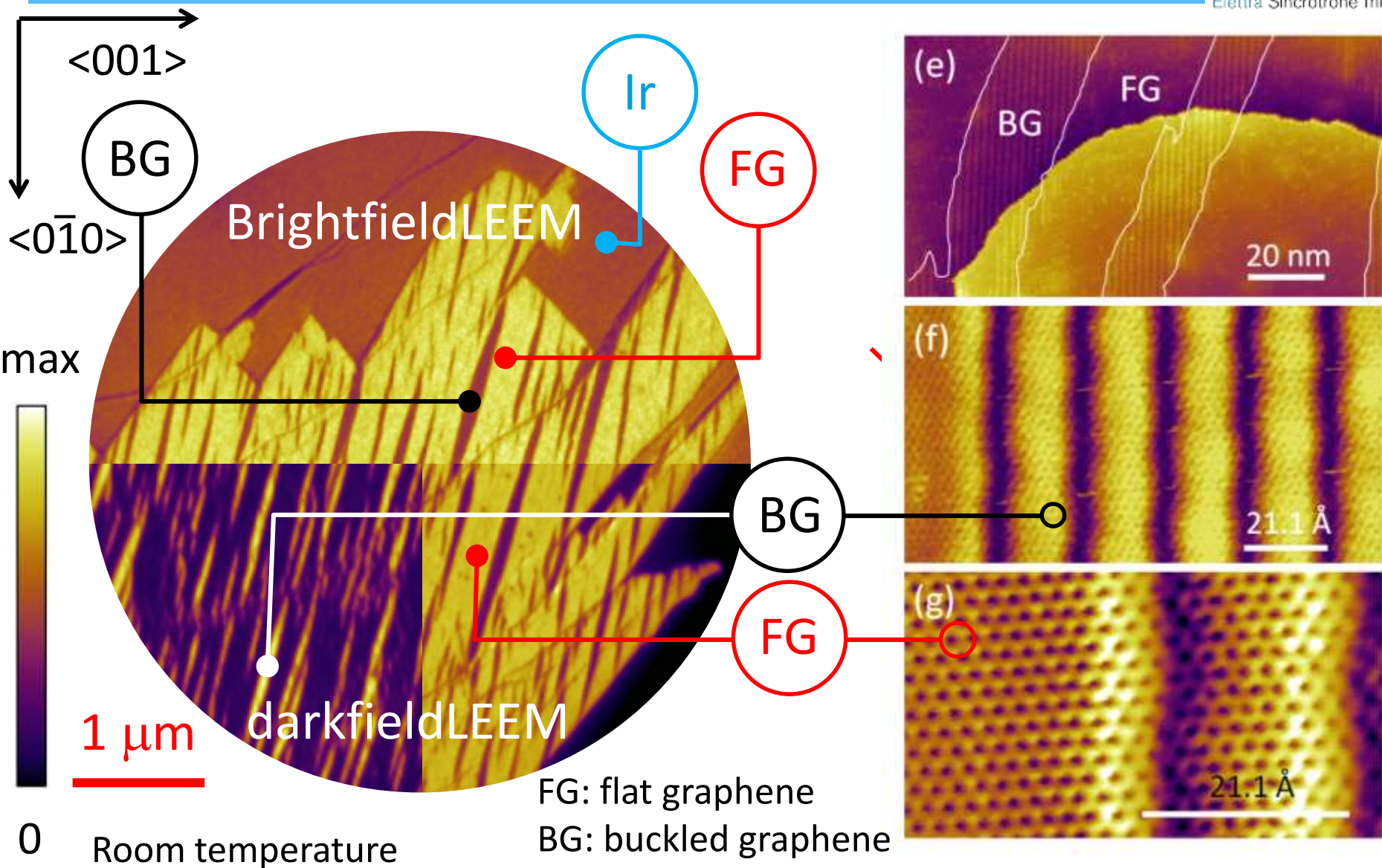# Reversible phase transformation in graphene

Upon cooling a new graphene phase nucleates (dark stripes)

The stripes disappear upon annealing to high temperature.

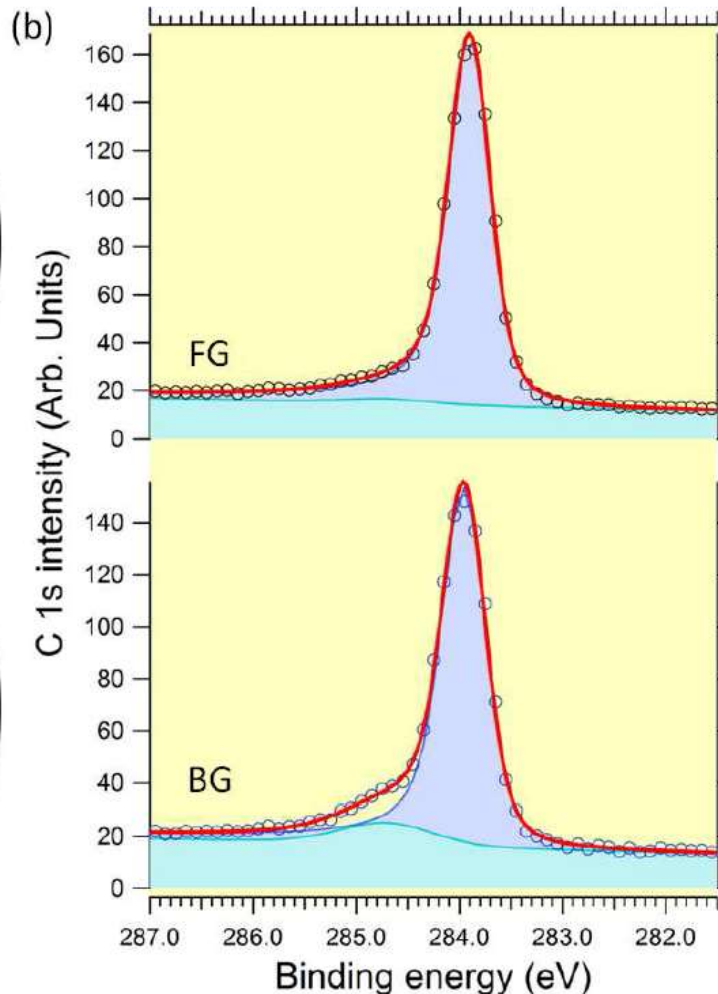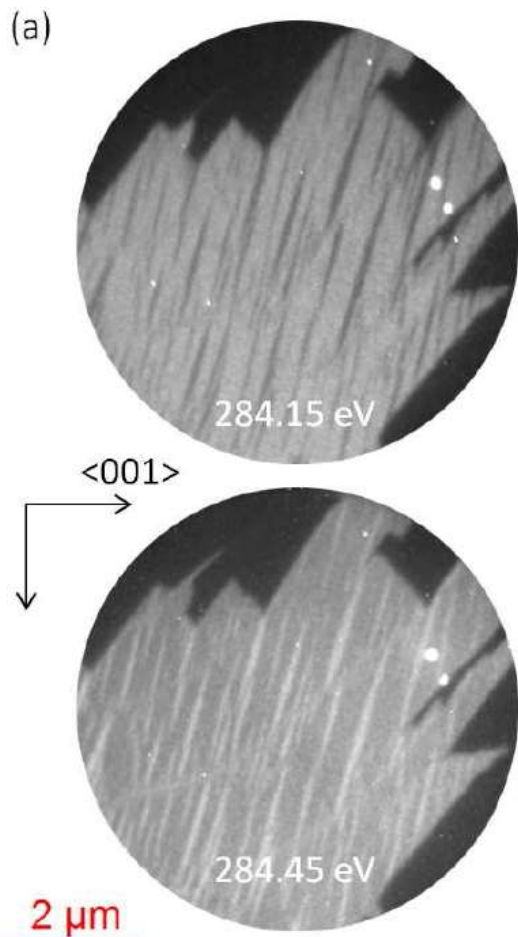# Graphene/Ir(100): strucutre of FG and BG

<001>

<0$\bar{1}$0>

BG

Ir

FG

BrightfieldLEEM

max

BG

FG

darkfieldLEEM

1 μm

0

Room temperature

FG: flat graphene
BG: buckled graphene

(e)

BG   FG

20 nm

(f)

BG

21.1 Å

(g)

FG

21.1 Å

Elettra Sincrotrone Trieste

Buckled graphene unit cell by ab-initio

buckled graphene unit cell

Buckled Graphene

Exceptionally large buckling

GGA:
❖ Min Ir-C distance of 1.9 Å
❖ Max Ir-C distance of 4.0 Å

DFT-D:
❖ Min Ir-C distance of 2.1 Å
❖ Max Ir-C distance of 3.7 Å

❖ 18 atoms over 160 (i.e. 11%) are **chemisorbed**, the others are physisorbed

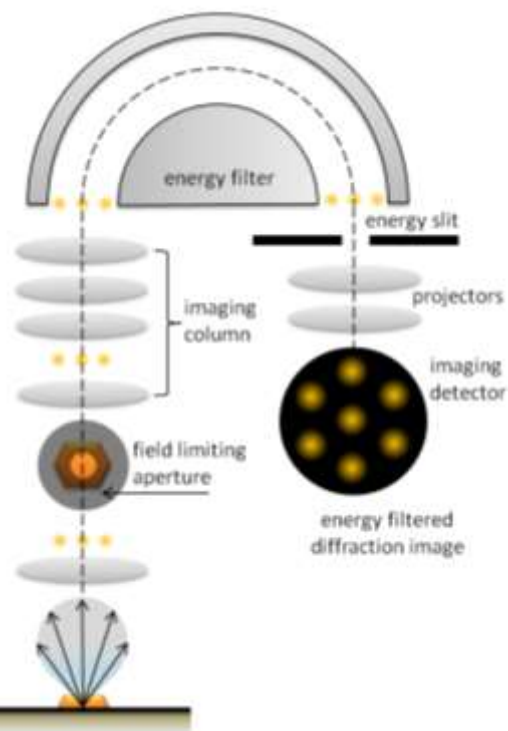**Buckled graphene shows regular one-dimensional ripples with periodicity of 2.1nm.**
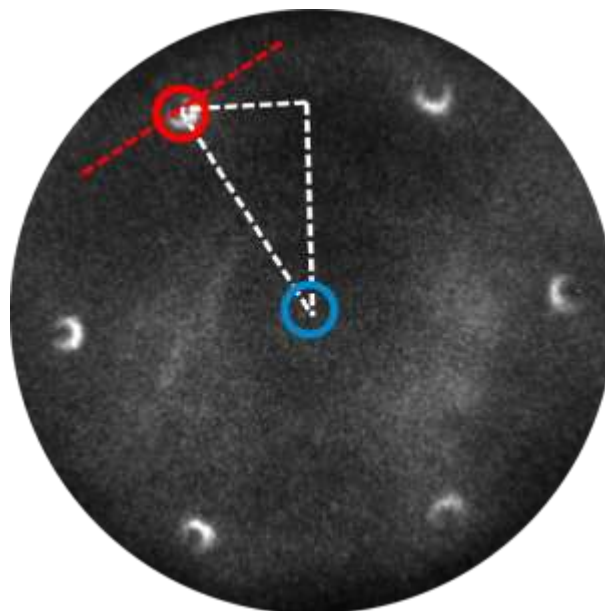
Electronic structure: graphene doping

what is the <u>difference in electronic structure</u> between FG and BG?
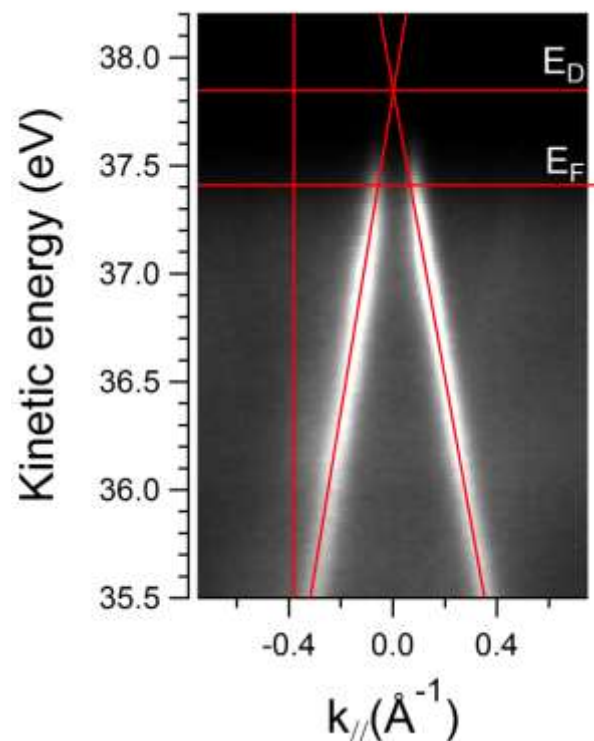do they both show the same Dirac-like dispersion?

Diffraction Imaging

measurements limited to
2 um in dia.

μ-ARPES at E_F

$E_D = 0.42$ eV

A. Locatelli et al; ACS Nano, ACS Nano, 7, 6955–6963 (2013)

Different character of FG and BG

dark-field
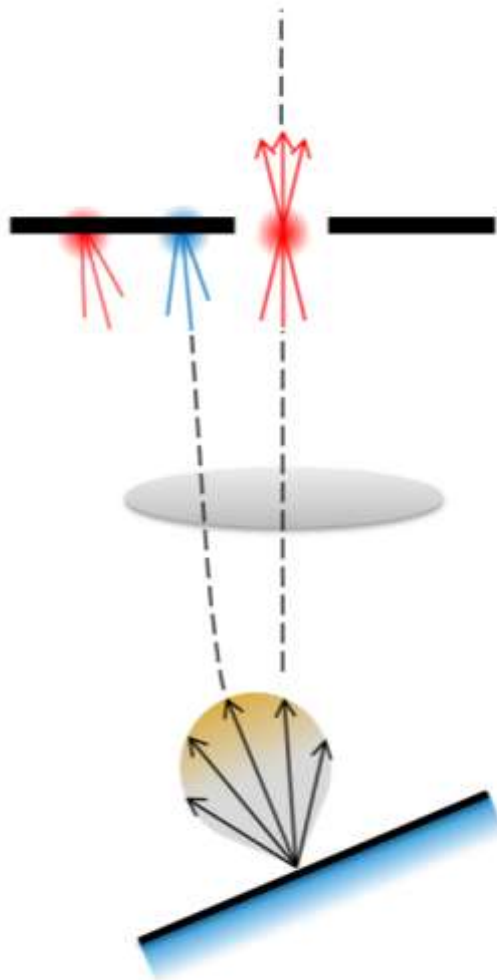
Image intensity proportional to local DOS!

BG

FG

Ir

df-XPEEM at K, E_F

2 µm
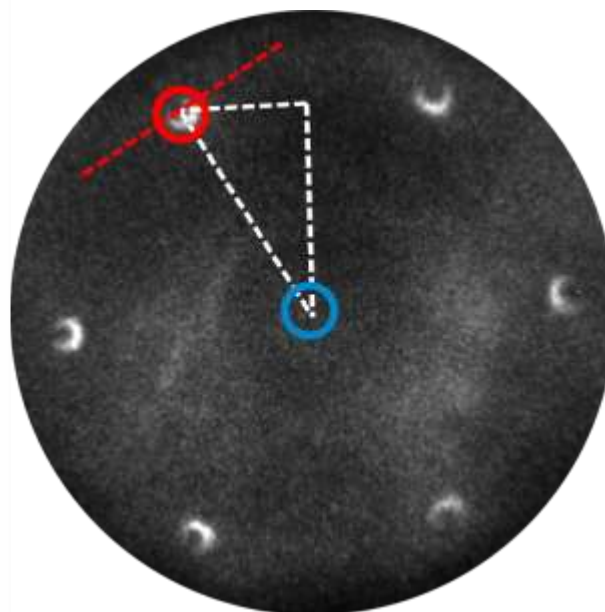
µ-ARPES at E_F
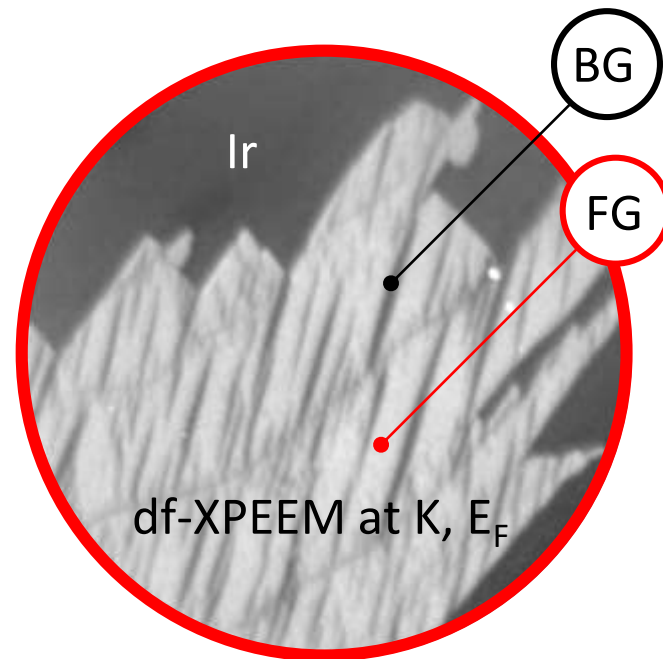
FG: high DOS at K → Dirac cones intact
BG hybridized, metalllic-like DOS

Decoupling graphene from substrate:

- **[Intercalated Au/g/Ir(100)]**

- **Switchable formation of carbides in g/Ni(111)**
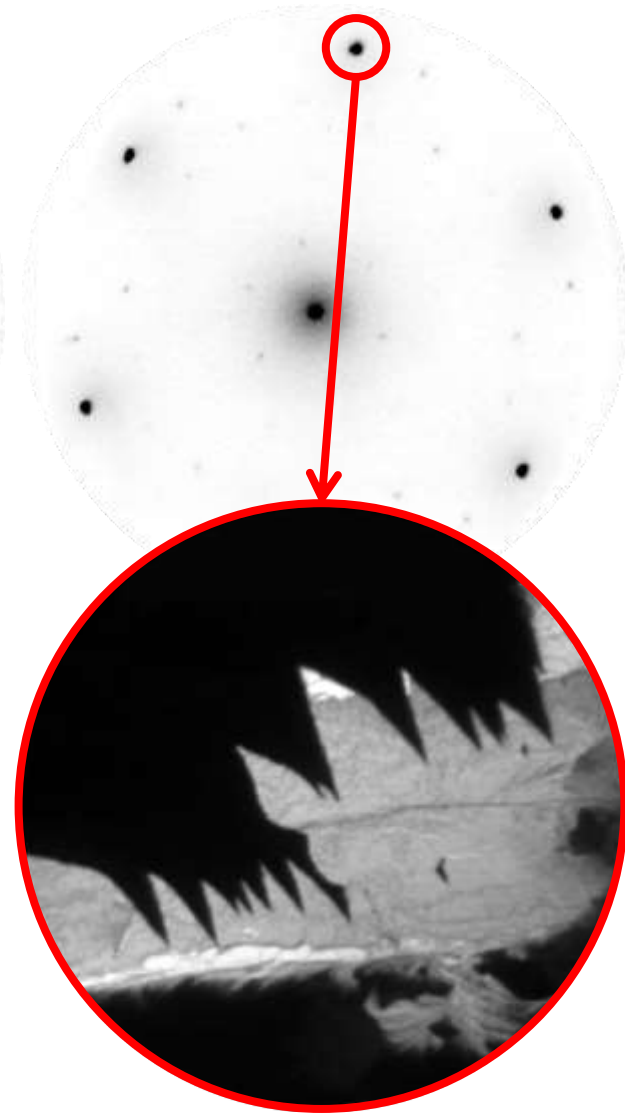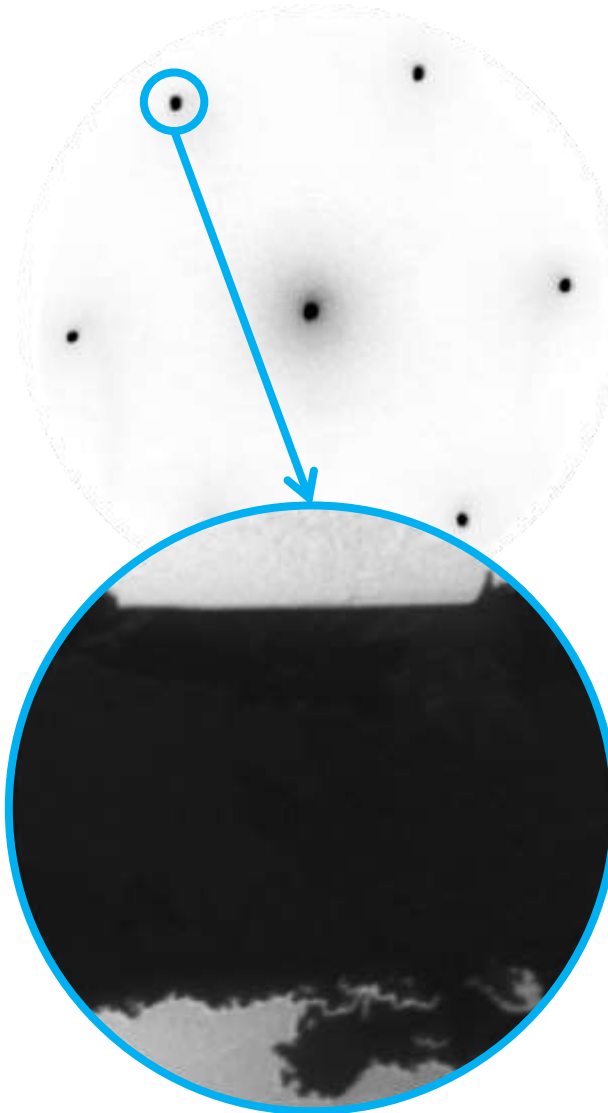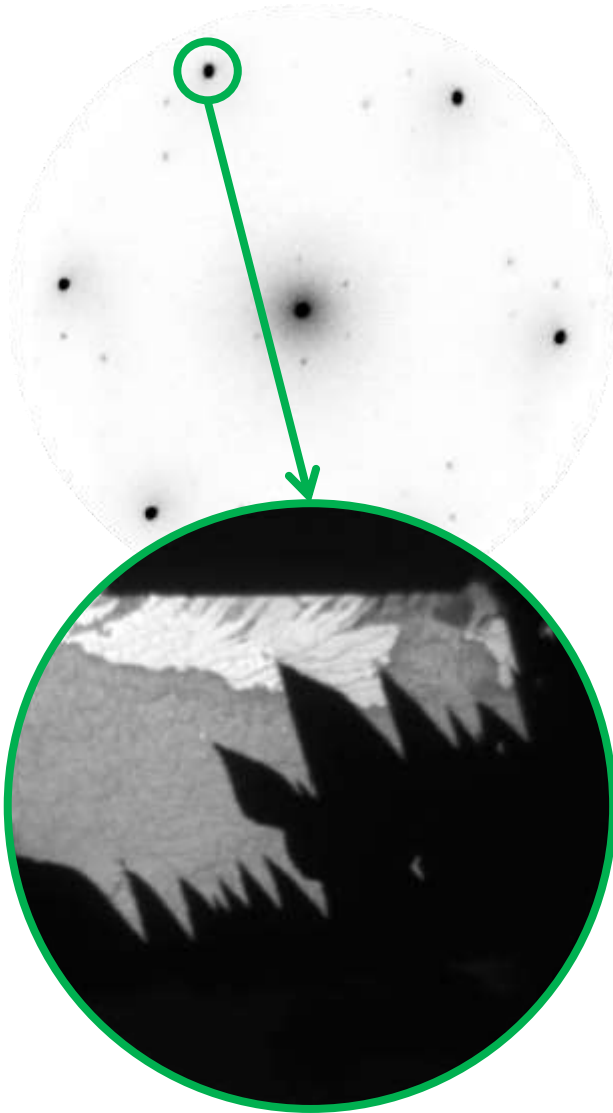
Identifying crystal grains in graphene/Ni(111)

rotated graphene (+17)   epitaxial graphene   rotated graphene (-17)

Formation/dissolution of carbides under rg/Ni(111)

1: carbide nucleation

380.41 C

1 µm

2: carbide growth

0.03 s

1 µm

3: carbide growth

262.04 C

1 µm
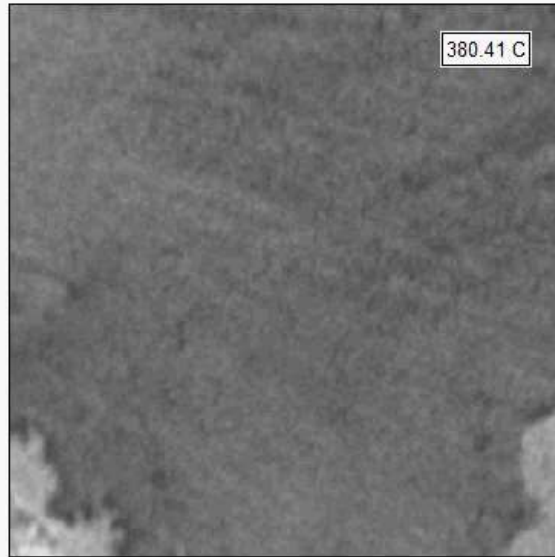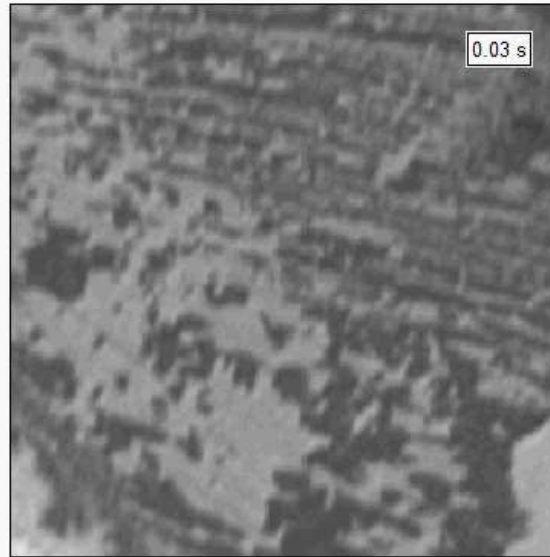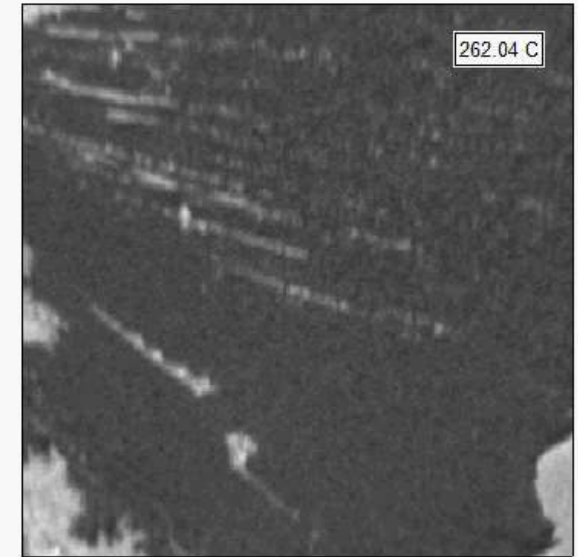
The Ni-carbide nucleates exclusively under rotated graphene, starting at temperatures below 340°C

A uniform layer of Ni-carbide is formed below graphene in about two hours

The carbide is dissolved into the bulk at about 360°C. The process is repeatable!

All movies: LEEM FoV 6 um, electron energy: 11 eV

C. Africh, C. Cepek, L.Patera. et al, Scientific Reports **6**, 19734 (2016)

Coupling-decoupling is revealed by µ-ARPES
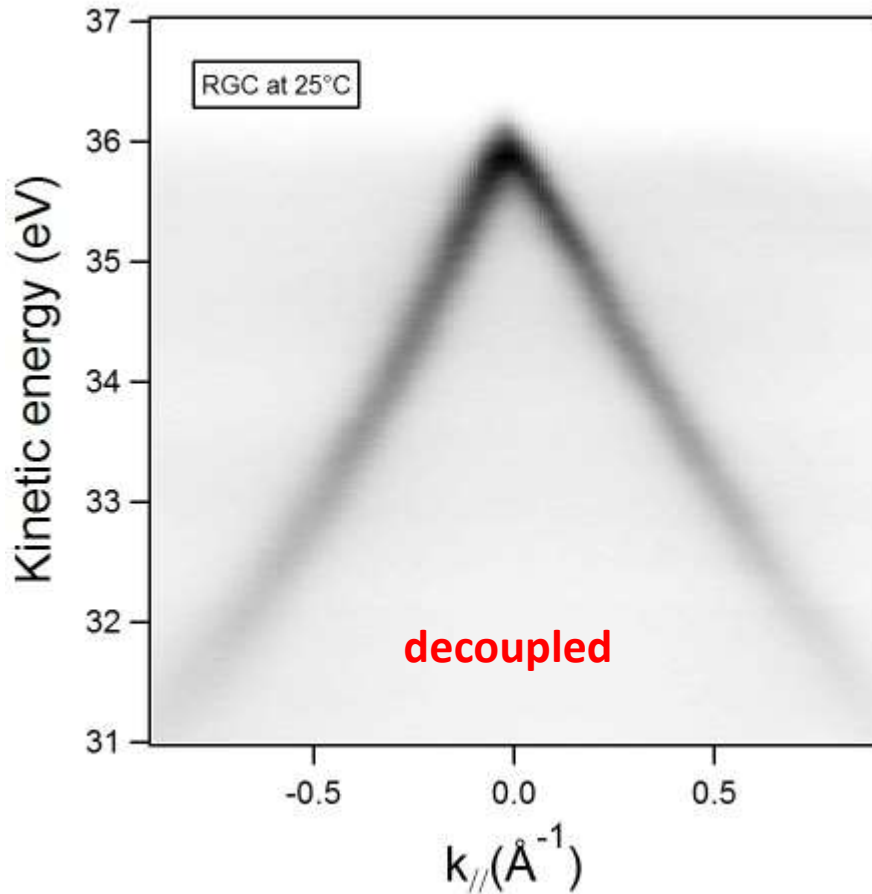
Rotated graphene with Ni-carbide
underneath at room temperature;
There's no double layer
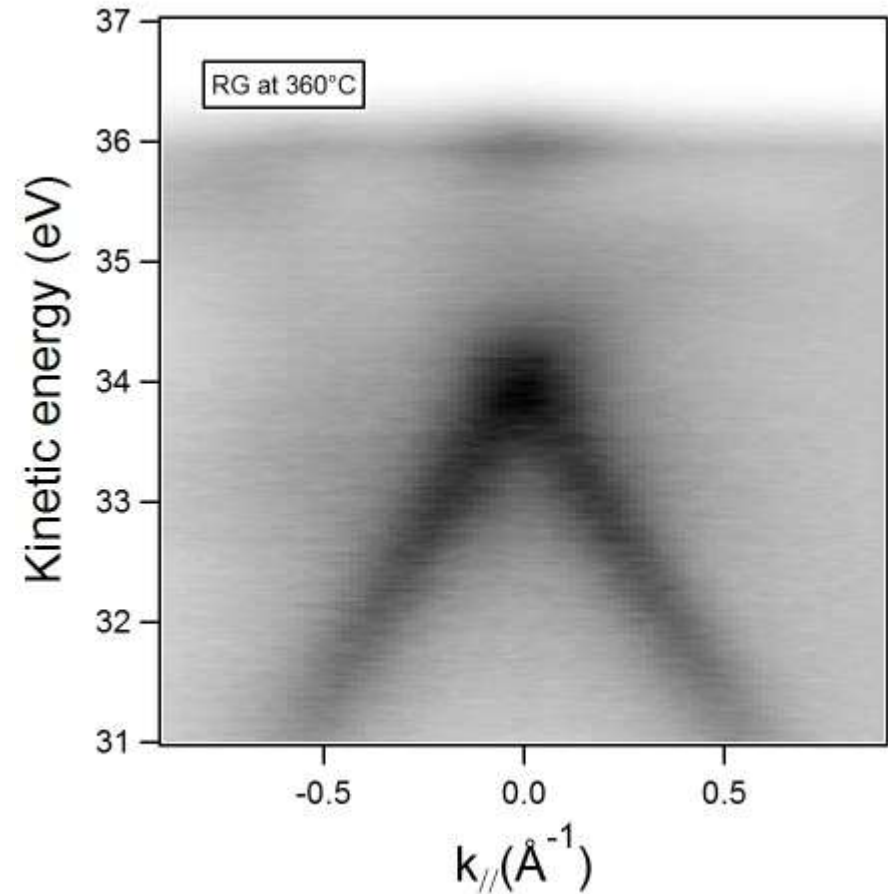
Rotated graphene without Ni-carbide
underneath at 365°C

C. Africh, C. Cepek, L.Paterq. et al, Scientific Reports **6**, 19734 (2016)

Ion irradiation of graphene

Nitrogen-ion irradiated gr/Ir(111)
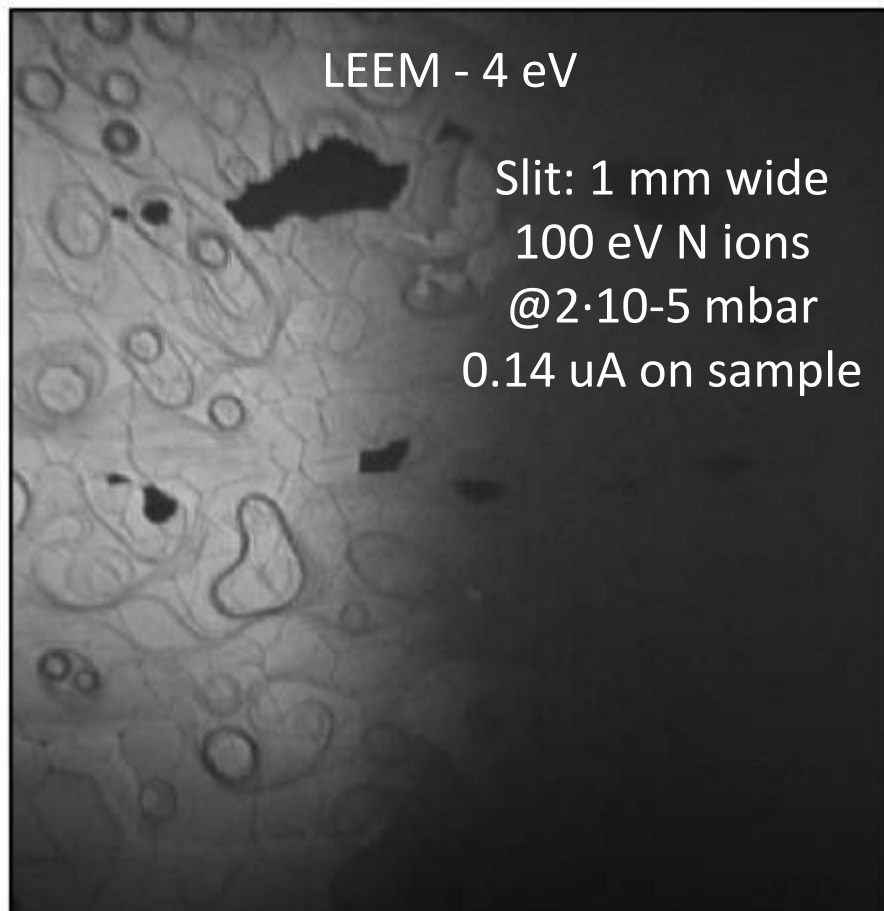
Nonirradiated   Irradiated

LEEM - 4 eV

Slit: 1 mm wide
100 eV N ions
@2·10-5 mbar
0.14 uA on sample

5 µm

Ion gun

N₂

Mask
Gr
Ir(111)

Nitrogen-ion irradiated gr/Ir(111)

Nonirradiated

Irradiated

LEEM - 4 eV

Slit: 1 mm wide
100 eV N ions
@2·10-5 mbar
0.14 uA on sample

XPEEM N 1s - 400.5 eV

5 µm

hν = 500 eV

Graphitic   Pyrrolic   Pyridinic

XPEEM N 1s

Nitrogen-ion irradiated gr/Ir(111)

A. Sala et al., Small 11(44), 5927-5931 (2015)

Applications of XAS in biology: biomineralization
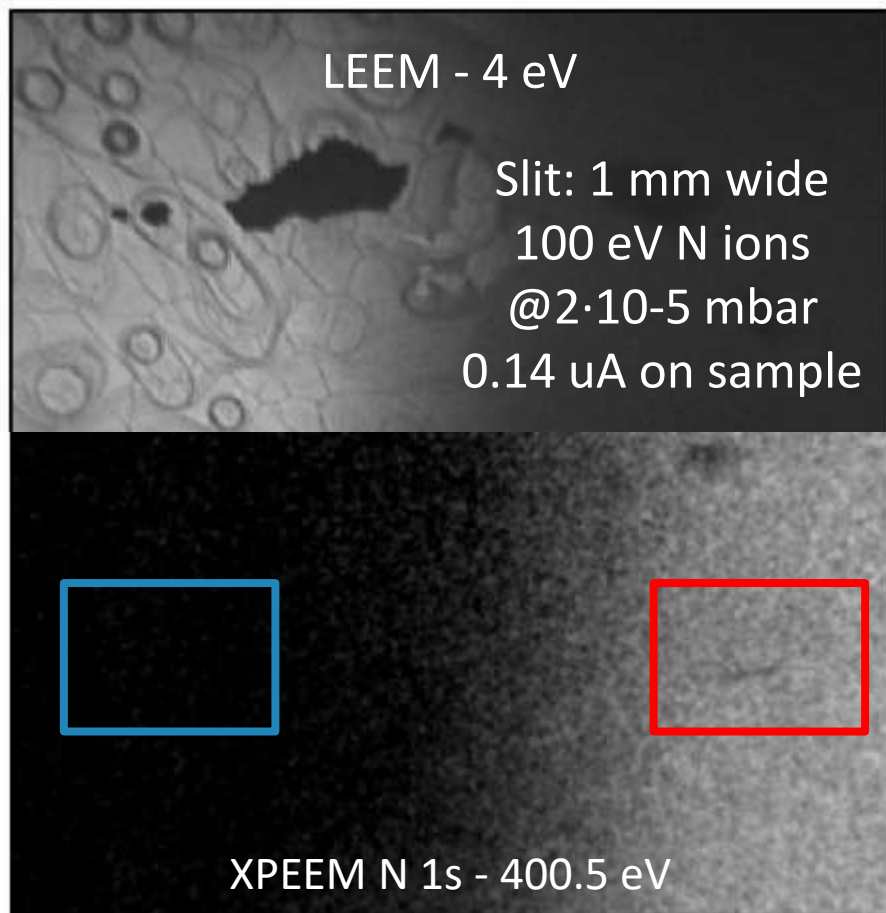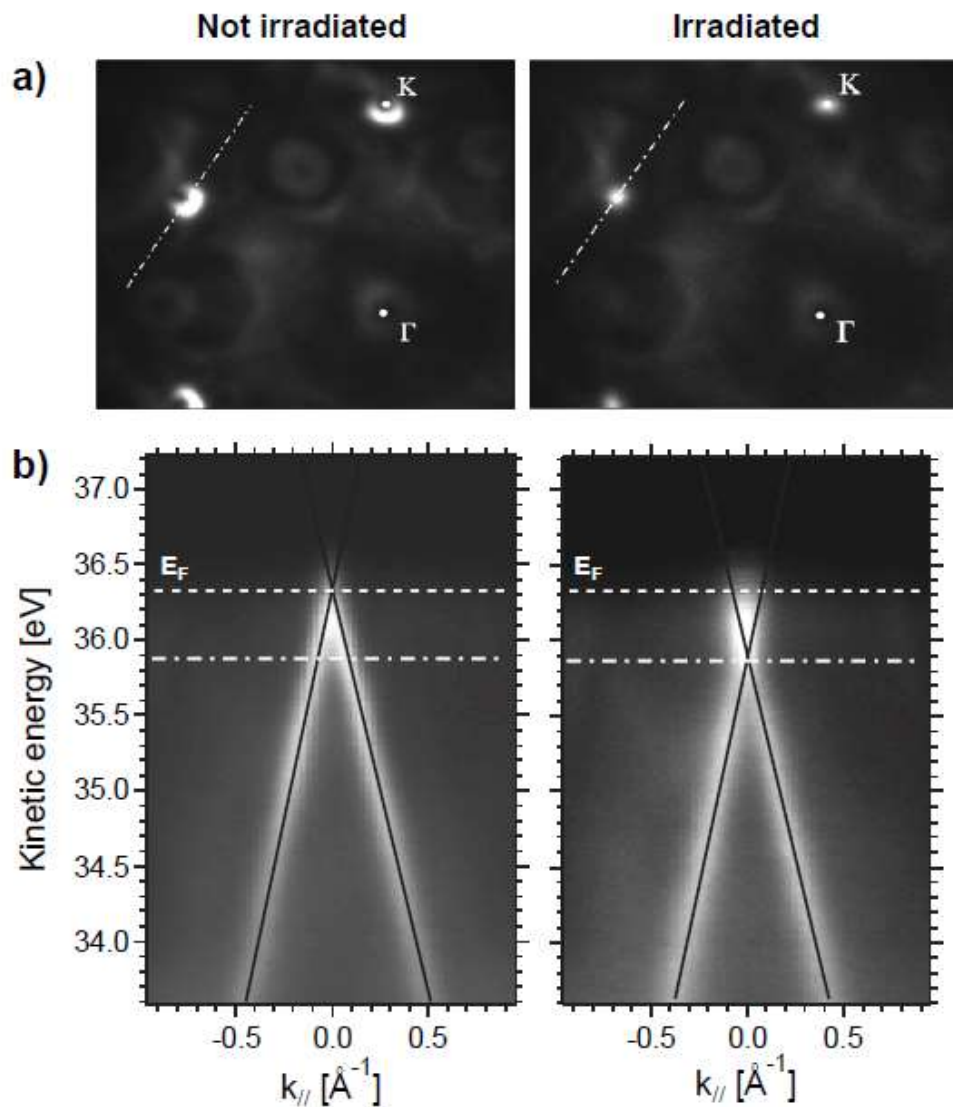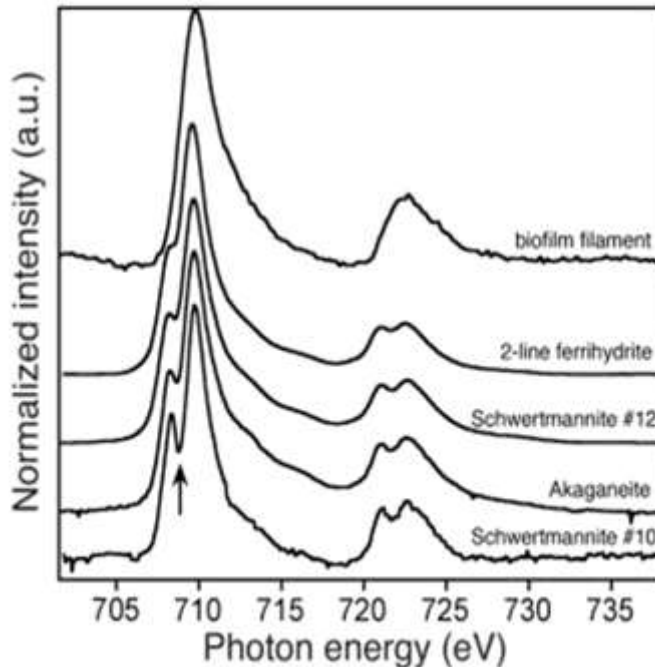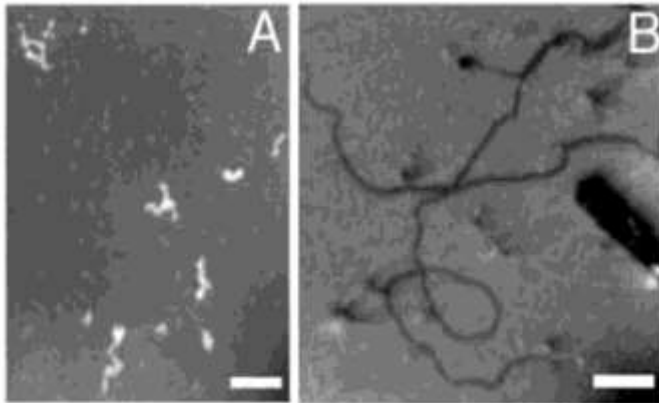
- Bio-mineralization resulting from microbal activity
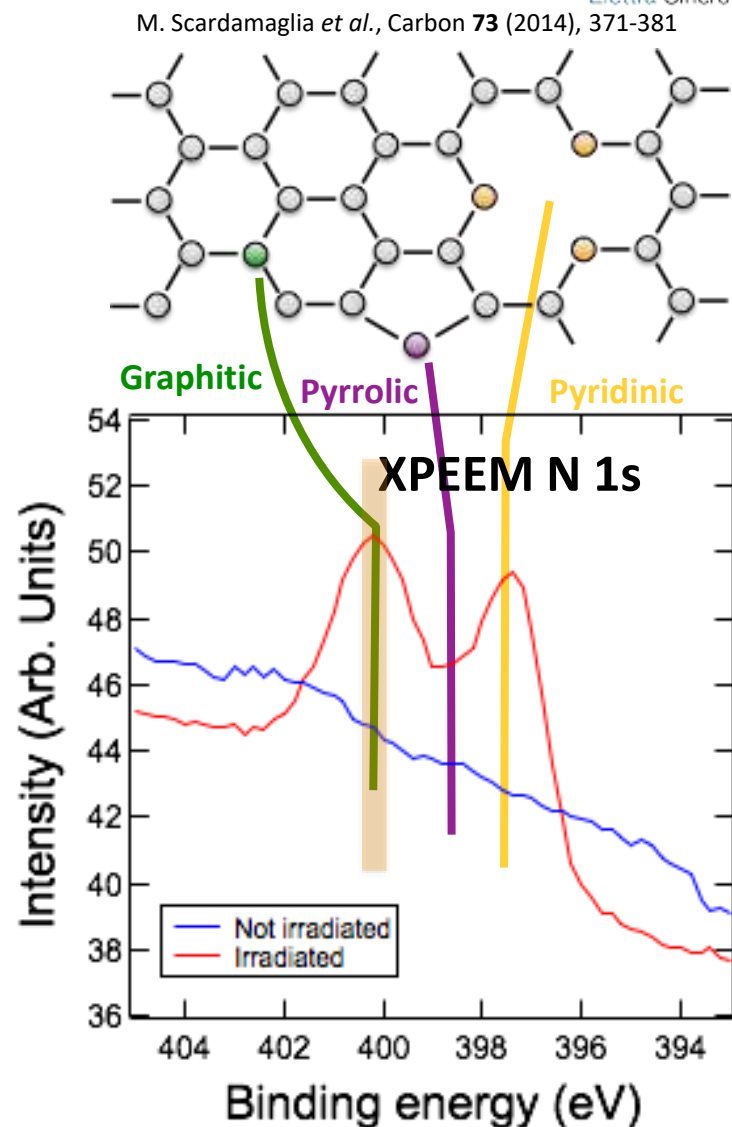- X-PEEM images of (A) non mineralized fibrils from the cloudy water above the biofilm (scale bar, 5 um)
- (B) mineralized filaments and a sheath from the biofilm (scale bar, 1 um); (bottom)
- X-PEEM Fe L-edge XANES spectra of the FeOOH mineralized looped filament shown in (B), compared with iron oxyhydroxide standards, arranged (bottom to top) in order of decreasing crystallinity.

P.U.P.A Gilbert *et al. (ALS group)*, *Science* **303** 1656-1658, 2004.

Nano-scale architecture of Nacre
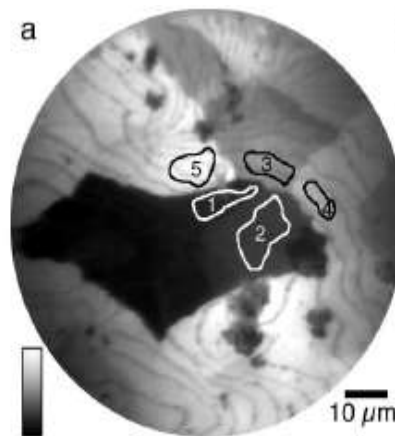
Carbon K-edge image

Carbon K-edge XANES

Oxygen K-edge XAS image

$$I(\vartheta, \theta, T) = a + b(3\cos^2\vartheta - 1)\langle Q_{zz}\rangle$$
$$+ c(3\cos^2\theta - 1)\langle M^2\rangle_T + d\sum_{i,j}\langle\hat{s}_i \cdot \hat{s}_j\rangle_T$$
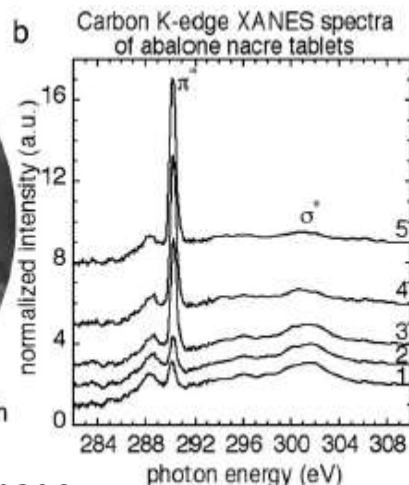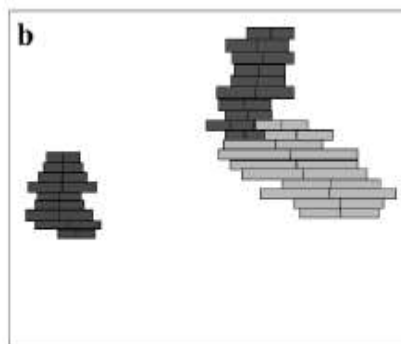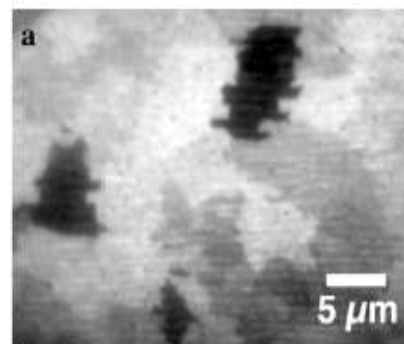
Contrast is observed between adjacent individual nacre tablets, arising because different tablets have different crystal orientations with respect to the radiation's polarization vector.

The 290.3 eV peak corresponds to the C 1s → Pi* transition of the CO bond. Synchrotron radiation is linearly polarized in the orbit plane. Under such illumination, the

intensity of the peak depends on the crystallographic orientation of each nacre tablet with respect to the polarization. This was the first observation of x-ray linear dichroism in a bio-mineral.

R.A. Metzler et al., Phys.Rev.Lett. **98**, 268102 (2007)

Part 3: XPEEM applications: magnetic imaging

Andrea Locatelli

Andrea.locatelli@elettra.eu

Why magnetism?

Topical Review

The 2017 Magnetism Roadmap

D Sander[1], S O Valenzuela[2,3], D Makarov[4], C H Marrows[5],
E E Fullerton[6], P Fischer[7,8], J McCord[9], P Vavassori[10,11], S Mangin[12],
P Pirro[13], B Hillebrands[13], A D Kent[14], T Jungwirth[15,16], O Gutfleisch[17],
C G Kim[18] and A Berger[10]

The change in landscape is hereby not exclusively scientific, but also reflects the magnetism related industrial application portfolio. Specifically, Hard Disk Drive technology, which still dominates digital storage and will continue to do so for many years, if not decades, has now limited its footprint in the scientific and research community, whereas significantly growing interest in magnetism and magnetic materials in relation to energy applications is noticeable, and other technological fields are emerging as well. Also, more and more work is occurring in which complex topologies of magnetically ordered states are being explored, hereby aiming at a technological utilization of the very theoretical concepts that were recognized by the 2016 Nobel Prize in Physics

Topics in Magnetism (i): materials

- **Novel two dimensional materials**
  - graphene, phosphorene, bismuth chalcogenides and transition metal dichalcogenides (TMDs) could play a key role for spintronics in a wide range of topics
  - Growth, mechanical assembly, self-assembly
  - Stacks/artificial FM/AFM materials, spin torque deivces, spin filters.
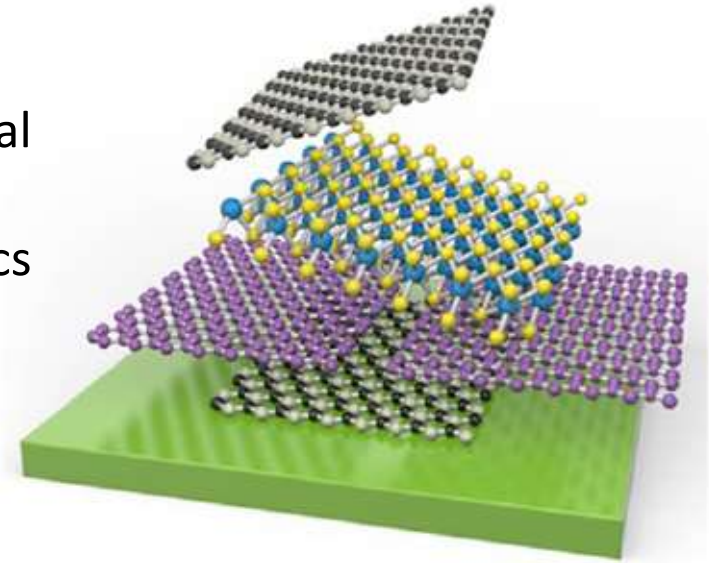
- **Novel materials with curved geometry:**
  - asymmetrically sandwiched ultrathin ferromagnetic metals, Heusler alloys, Weyl semimetals, and magnetoelectric materials.
  - Topological structures (chiral, e.g. skyrmions)

Gr
Co

Topics in Magnetism (ii): materials

(a)

-1 m_z 1

(b)

Gr
Co

- **Novel materials with curved geometry:**
  - asymmetrically sandwiched ultrathin ferromagnetic metals, Heusler alloys, Weyl semimetals, and magnetoelectric materials.
  - Topological structures (chiral, e.g. skyrmions)

Magnetic imaging methods: an overview
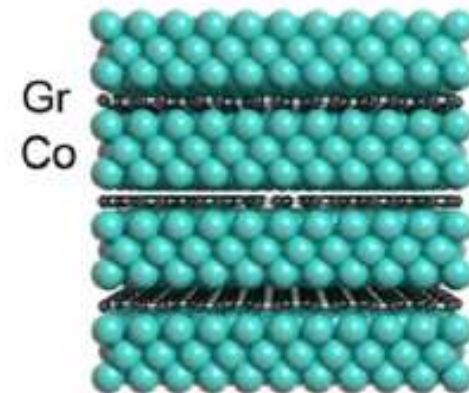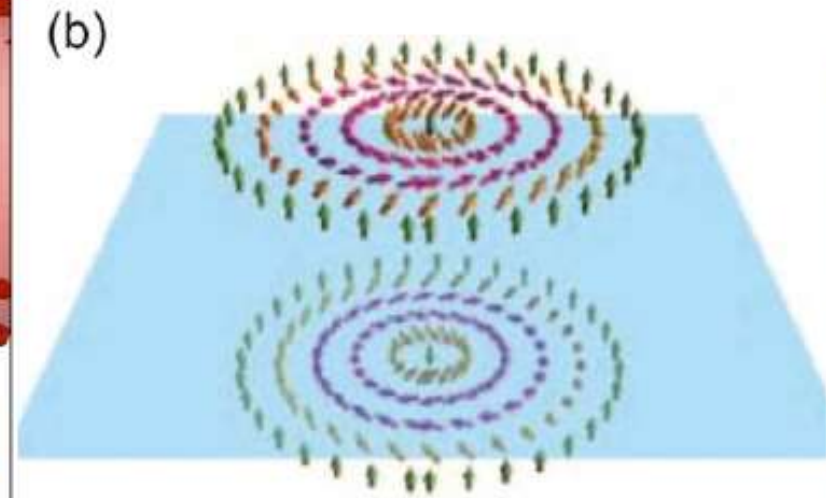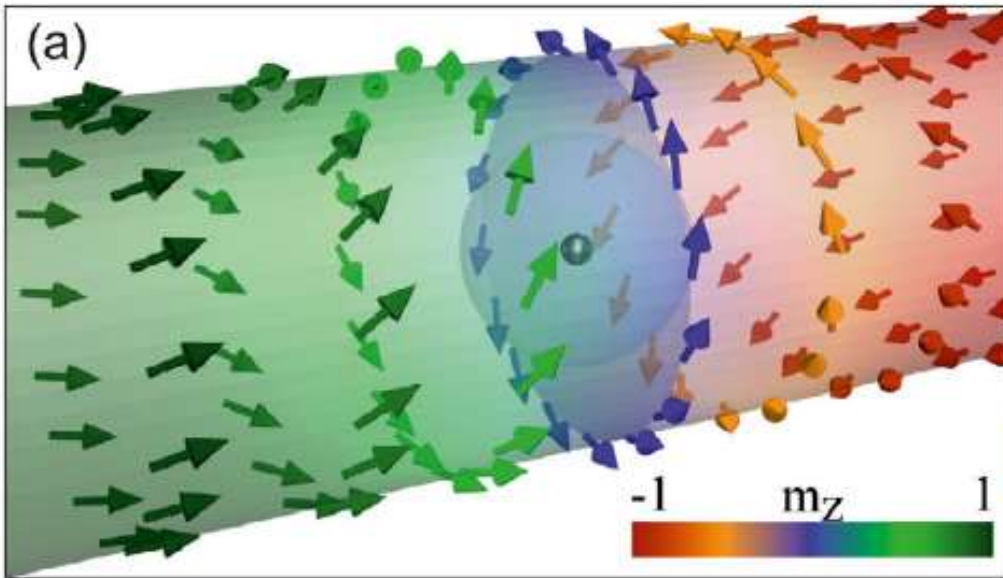
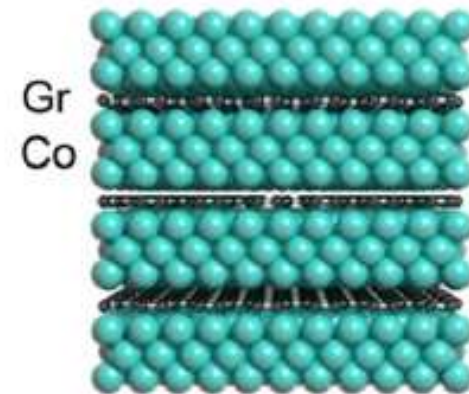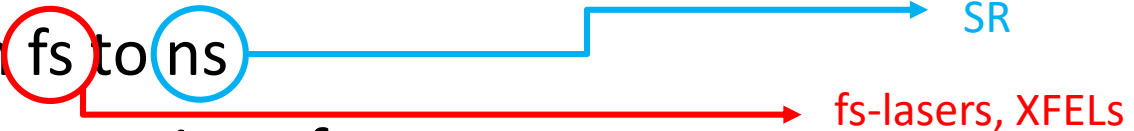The direct mapping of individual non-collinear spin textures with atomic precision is a formidable experimental challenge. Transmission electron microscopy with Lorentz imaging (Lorentz-TEM) of magnetic order [6], magnetic force microscopy (MFM) [7], secondary electron microscopy with polarization analysis (SEMPA) [8], photoemission electron microscopy (PEEM) [9], spin-polarized scanning tunneling microscopy (spin-STM) [3] and spin-polarized low energy electron microscopy (SPLEEM) [10] are established, highly specialized experiments to tackle this task. Among these techniques only the first two could retrieve the magnetization information from a buried layer, whereas the high surface sensitivity of the last three techniques renders them most useful for characterizing exposed magnetic structures under ultra-high vacuum conditions. Magneto-optical Kerr effect (MOKE) (see section 7) is a powerful technique to characterize the dynamics of non-collinear spin structures, including skyrmion formation [11].

- Magneto-optical microscopies (MOKE)
- Magnetic scanning probe microscopies (MFM)
- Magnetic electron microscopies (SEMPA, SPLEEM)
- **Magnetic x-ray microscopies (STXM, PEEM)**

- Imaging the magnetic state of the material, e.g. understanding the magnetic domain structure with nm lateral resolution

- Monitoring its evoultion under an external stimulus. This requires both space and time resolution!

Magnetic imaging methods: requirements!

- Lateral resolution close to the nm
- Time resolution: from fs to ns
- Sensitivity to buried layers, interfaces
- Ability to quantify mangnetic properties!
- in-operando studies:

  as a function of external parameters,
  magnetic and electric fields,
  current pulses,
  temperature, pressure (under UHV, or in gases)
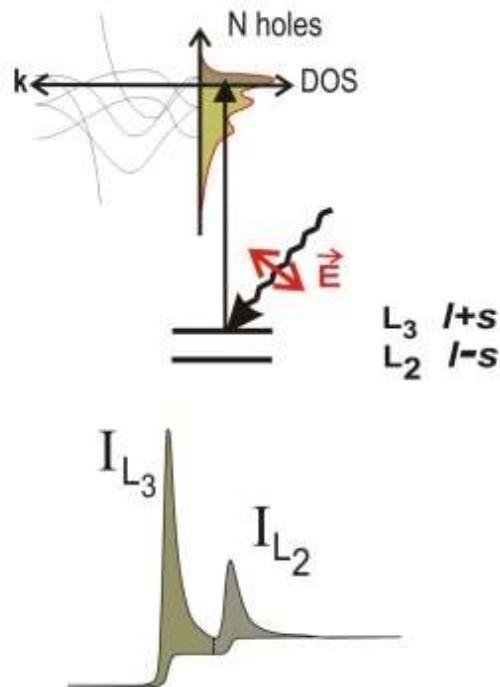 Control of strain (magneto-electrics in multifferroic materials)

SR

fs-lasers, XFELs

J. Phys. D: Appl. Phys. **50** (2017) 363001

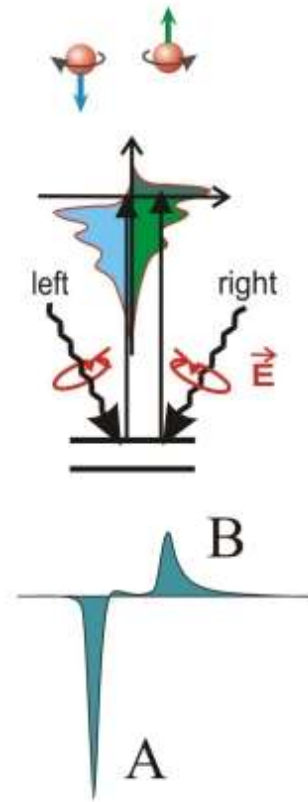## 6. Advances in magnetic characterization

Peter Fischer[1]

Using electric fields to switch magnetization in multiferroic materials, utilizing pure spin currents or at least spin polarized currents in spin-orbitronics, and ultimately all-optical control of magnetism are the most prominent research directions today (section 9). The challenges for characterization are the ability to study with high spatial and temporal resolution, ultimately down to the nm and fs regimes, respectively, and in–operando as a function of applied external parameters, including electric and heat currents, electric and magnetic fields, ultrashort optical pulses, the statics and dynamics of the underlying microscopic spin textures. A detailed, i.e. highly spatial, and temporal resolution characterization of spin textures at buried interfaces and specifically the spin dynamics at such interfaces, or more generally, the behavior of spins in 3D nanoscale systems, is still elusive. Whereas, independently, fundamental
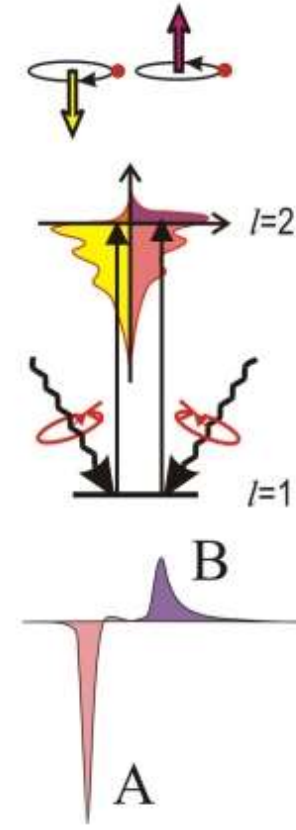
XMCD principles

(a) d-Orbital Occupation   (b) Spin Moment   (c) Orbital Moment

The spin-split valence shell is a detector for the spin of the excited photoelectron.

Sum rules

- intensity of the L_3 and L_2 goes with empty d states (holes).
- Size of spin and orbital moments

J. Stoehr et al., IBM. J . Res. Develop. 42, 73 (1998) and J. Magn. Magn. Mater. 200, 470 (1999).

Magnetic domain imaging by XMCD
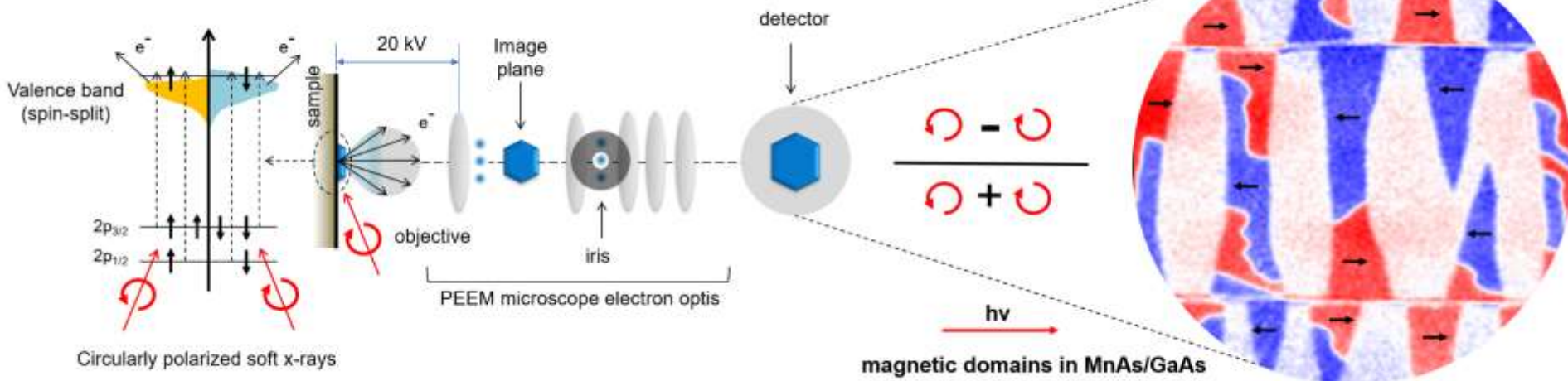
(a) magnetic circular dichroism

(b) Photoemission electron microscope (PEEM)

(c) Microscopy with magnetic sensitivity

Valence band (spin-split)

20 kV

Image plane

detector

$2p_{3/2}$
$2p_{1/2}$

objective

iris

PEEM microscope electron optis

Circularly polarized soft x-rays

hv

magnetic domains in MnAs/GaAs

- The x-ray <u>absorption</u> depends on the <u>relative orientation</u> of the <u>magnetization</u> and the <u>polarization</u> of circularly polarized light.
- The size of the dichroism effect scales like cos(θ)
- We **PROBE** 3d elements by exciting 2p into unfilled 3d states
- Photoelectrons with opposite spins are created in the cases of left and right handed polarization.
- Spin polarization is opposite for $p_{3/2}$ (L$_3$) and $p_{1/2}$ (L2) levels.

Elettra Sincrotrone Trieste

**Experimental Confirmation of the X-Ray Magnetic Circular Dichroism
Sum Rules for Iron and Cobalt**

PRL 75, 152; 1995

C. T. Chen,[1] Y. U. Idzerda,[2] H.-J. Lin,[1,*] N. V. Smith,[1,†] G. Meigs,[1] E. Chaban,[1]
G. H. Ho,[3,*] E. Pellegrin,[1] and F. Sette[1,‡]

SUM RULES

$$m_{orb} = -\frac{4 \int_{L_3+L_2}(\mu_+ - \mu_-)\, d\omega}{3 \int_{L_3+L_2}(\mu_+ + \mu_-)\, d\omega}(10 - n_{3d}), \quad (1)$$

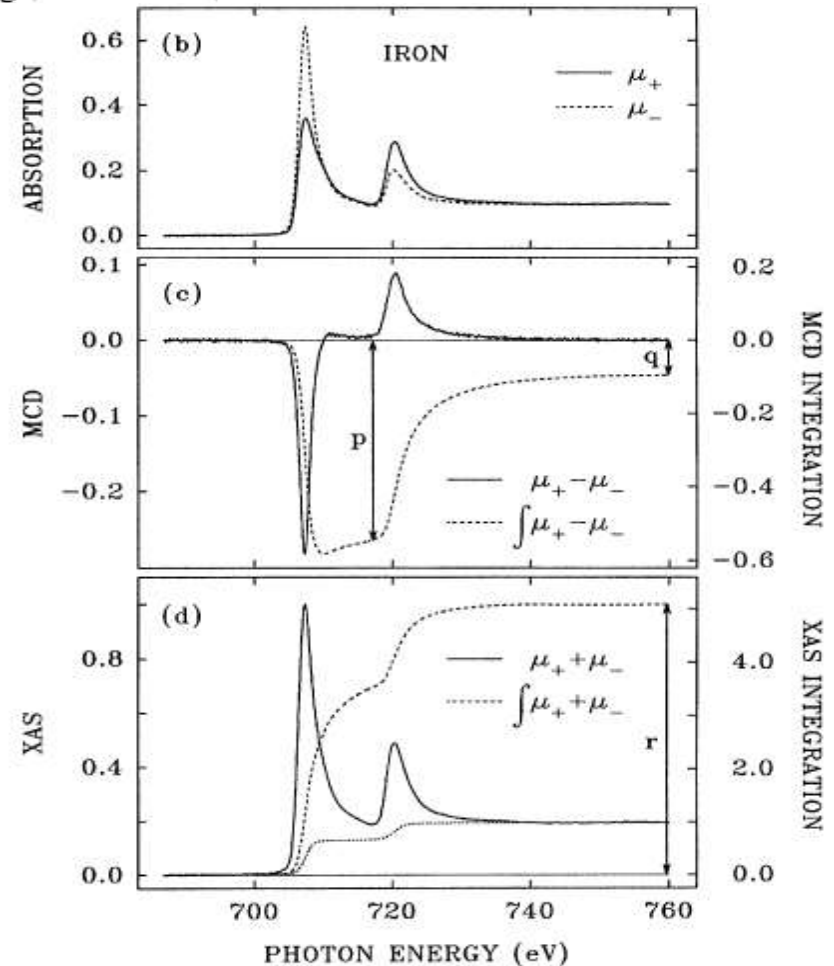$$m_{spin} = -\frac{6 \int_{L_3}(\mu_+ - \mu_-)\, d\omega - 4 \int_{L_3+L_2}(\mu_+ - \mu_-)\, d\omega}{\int_{L_3+L_2}(\mu_+ + \mu_-)\, d\omega}$$
$$\times (10 - n_{3d})\left(1 + \frac{7\langle T_z\rangle}{2\langle S_z\rangle}\right)^{-1}, \quad (2)$$

$\langle T_z\rangle$ is the expectation value of the magnetic
dipole operator

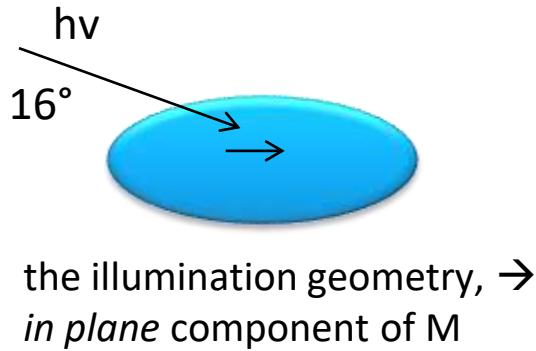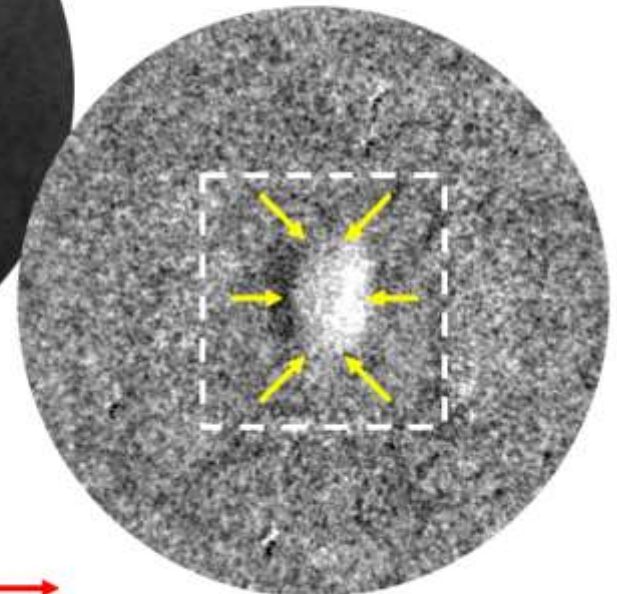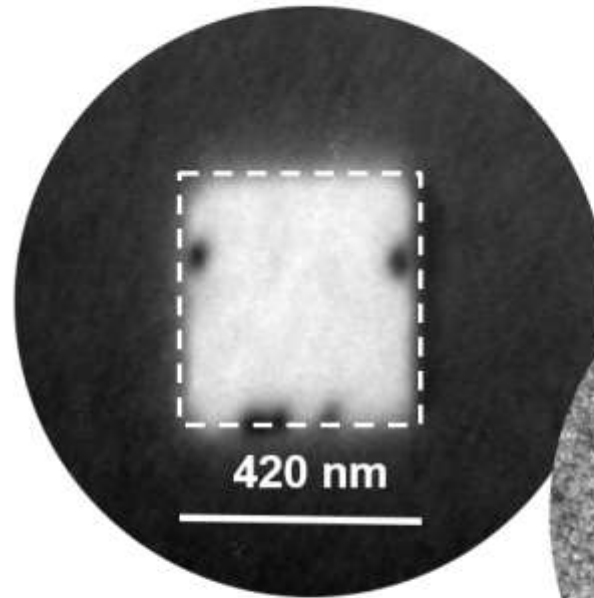$\langle S_z\rangle$ is equal to half of m_{spin}

REFERENCES

B. T. Thole, P. Carra, F. Sette, and G. van der Laan, Phys. Rev. Lett.
68, 1943 (1992); P. Carra, B. T. Thole, M. Altarelli, and X.Wang,
Phys. Rev. Lett. 70, 694 (1993), J.Stöhr et al, Phys. Rev. Lett. 75
(1995) 3748.

XMCD imaging of a skyrmion

hv

16°

the illumination geometry, →
in plane component of M

(d) Chemical image of a magnetic nanostructure

420 nm

(e) Magnetic image of a skyrmion

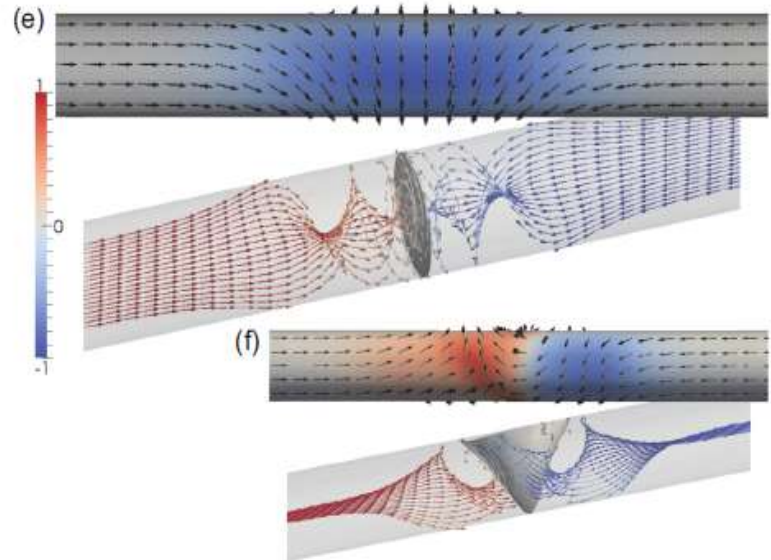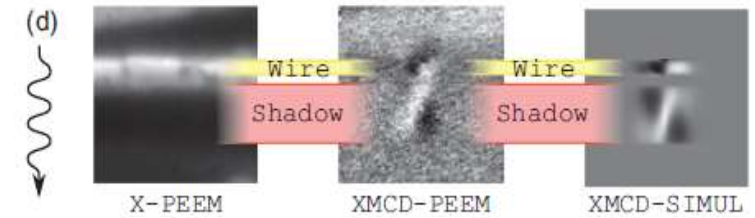O. Boulle et al., Nat. Nanotech. **11**, 449–454 (2016)

Tomographic imaging in magnetic wires

Observation of Bloch-point domain walls in cylindrical magnetic wir

S. Da Col *et al*., Phys. Rev. B**89**, 180405(R) (2014)
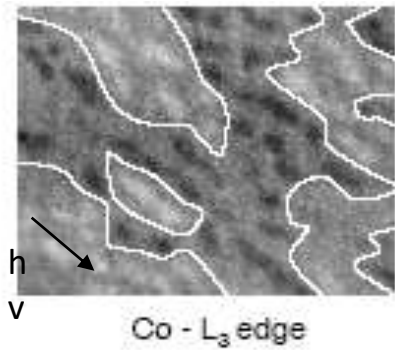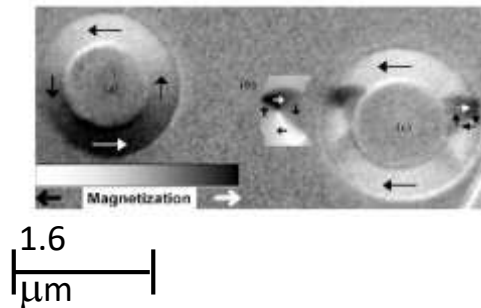
Examples of XMCD-PEEM applications
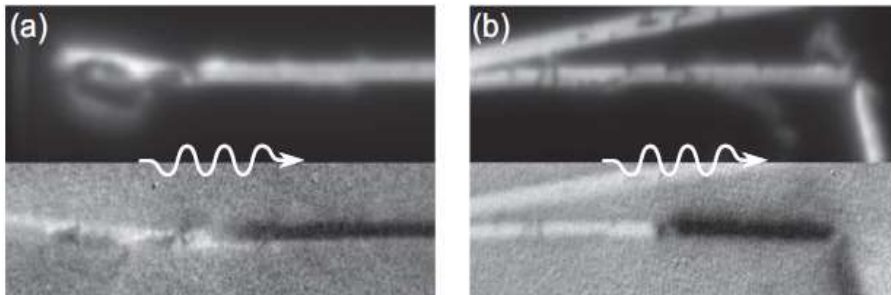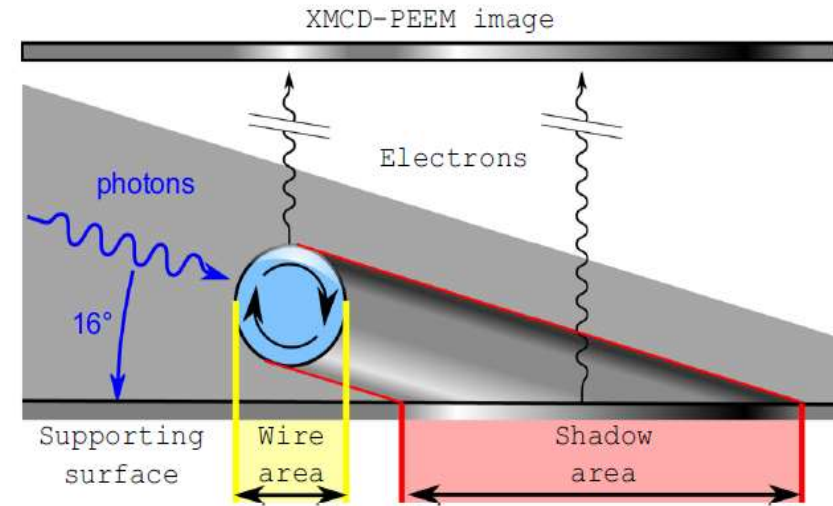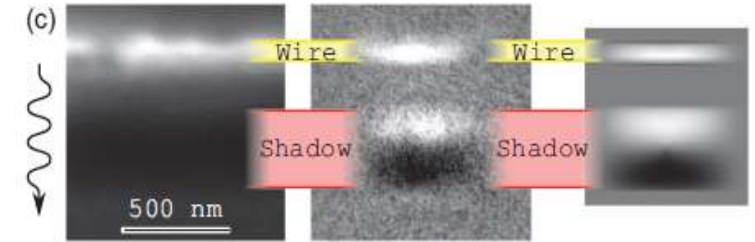
IMAGING OF MAGNETIC DOMAINS & DOMAIN WALLS
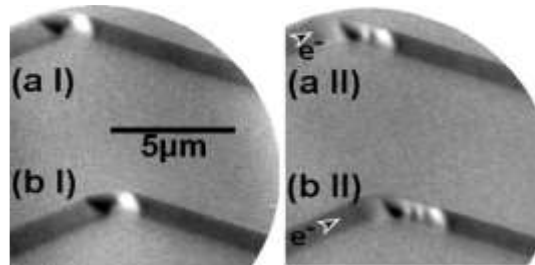
Co nanodots on Si-Ge

Co - L$_3$ edge

A. Mulders et al, Phys. Rev. B 71, 214422 (2005).

patterned structures

1.6 μm

pulse injection

M. Klaeui et al, PRL , PRB 2003 - 2010

domain wall motion induced by spin currents
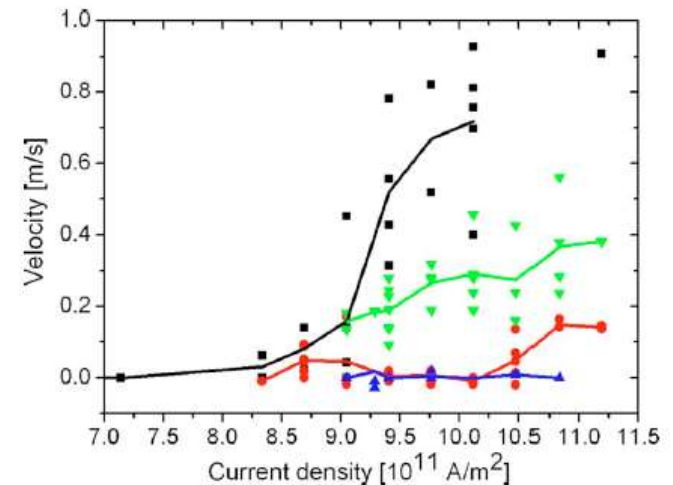
Laufemberg et al, APL 88, 232507(2006).

Limited probing depth of XMCD: MnAs/GaAs

Experiment: Straight walls; Head to head domains

180 nm
MnAs
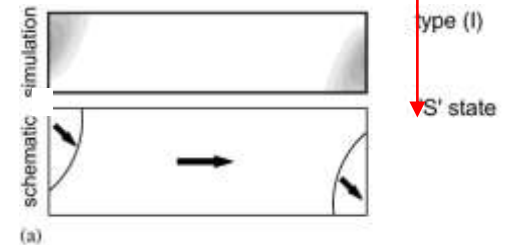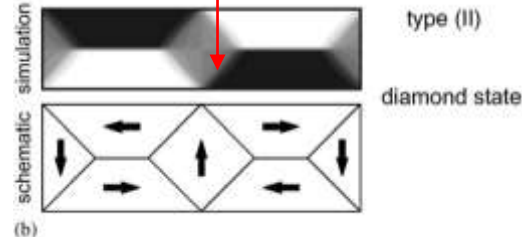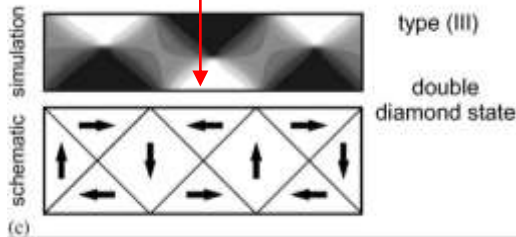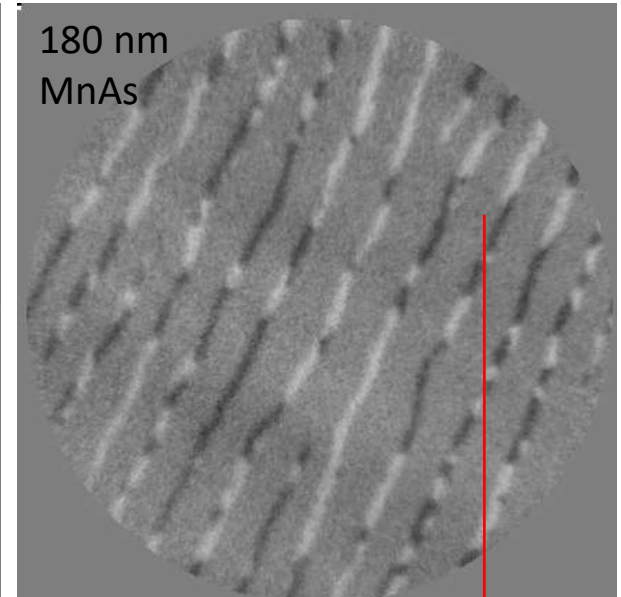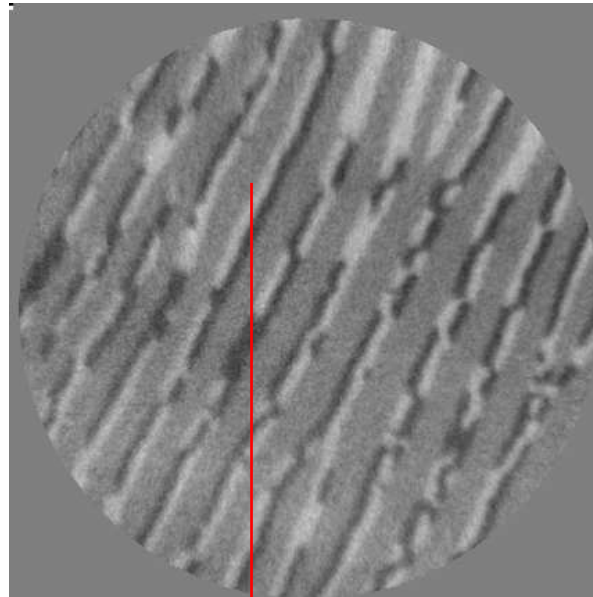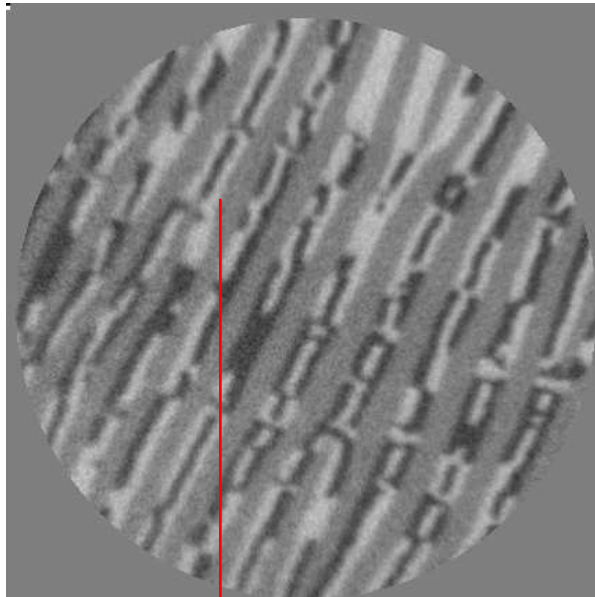
Simulation: Cross sectional cut: diamond state

R. Engel-Herbert et al, J. Magn. Magn. Mater. 305, (2006) 457

Samples fabrication issues

- In situ prepared
  - grow your own samples! (e-beam evaporation/lengthy)
  - Surface science approach
- Ex-situ prepared
  - complex multilayers (MBE facility)
  - Advanced lithography
  - Issue: contaminations due to exposure to atmosphere / capping layers needed
  - Contacting nanostructures

Magnetic imaging basics: XMLD

Linear Dichroism - Antiferromagnets
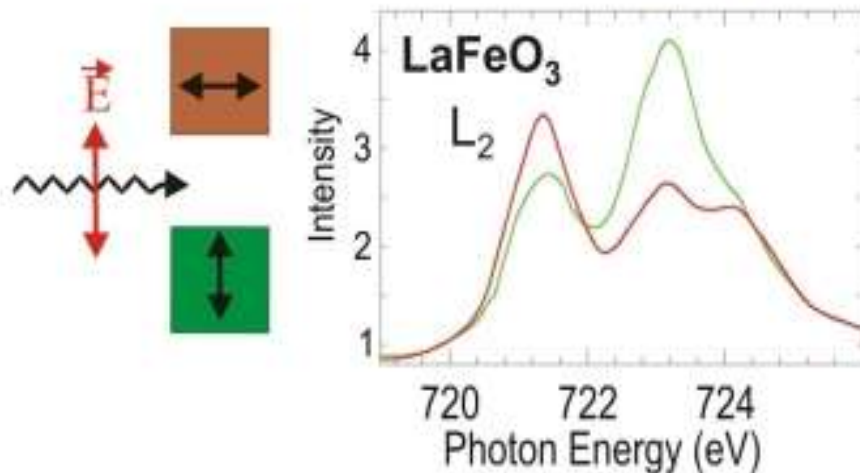
In the presence of spin order the spin-orbit coupling leads to preferential charge order relative to the spin direction, which is exploited to determine the spin axis in antiferromagnetic systems.

✓Element sensitive technique

✓ Secondary imaging with PEEM determine large probing depth (10 nm), buried interfaces.

✓Applied in AFM systems (oxides such as NiO)

Absorption intensity at resonance

$$I(\vartheta, \theta, T) = a + b(3\cos^2\vartheta - 1)\langle Q_{zz}\rangle$$

$$+ c(3\cos^2\theta - 1)\langle M^2\rangle_T + d\sum_{i,j}\langle \hat{s}_i \cdot \hat{s}_j\rangle_T$$

1st term: quadrupole moment, i.e.electronic charge (not magnetic!)

2nd term determines XMLD effect; θ is the angle between E and magnetic axis A; XMLD max for E || A;
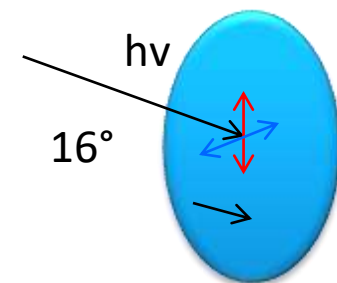
Linear vertical and linear horizontal polarization of the photon beam

Direct observation of the alignment of ferromagnetic spins by antiferromagnetic spins

F. Nolting*, A. Scholl*, J. Stöhr†, J. W. Seo‡§, J. Fompeyrine§,
H. Siegwart§, J.-P. Locquet§, S. Anders*, J. Lüning†, E. E. Fullerton†,
M. F. Toney†, M. R. Scheinfein‖ & H. A. Padmore*

ferromagnet/antiferromagnet
Co/LaFeO3 bilayer
interface exchange coupling
between the two materials

LaFeO$_3$ layer
XMLD Fe L$_3$

Co layer
XMCD Co L$_3$/L$_2$

Normalized Intensity (a.u.)
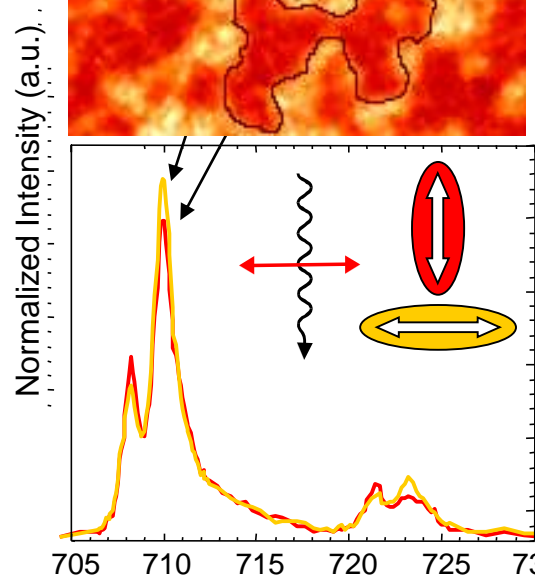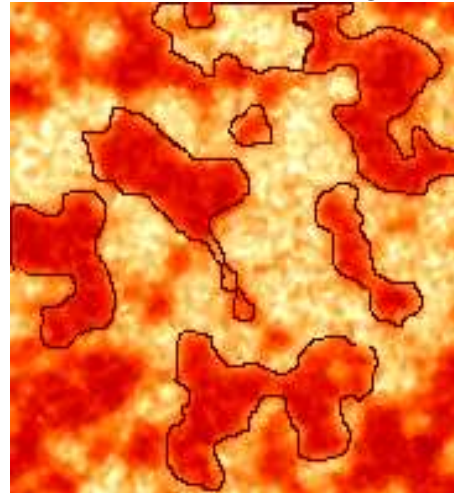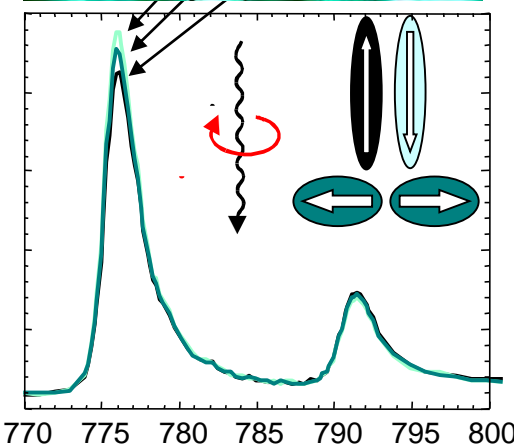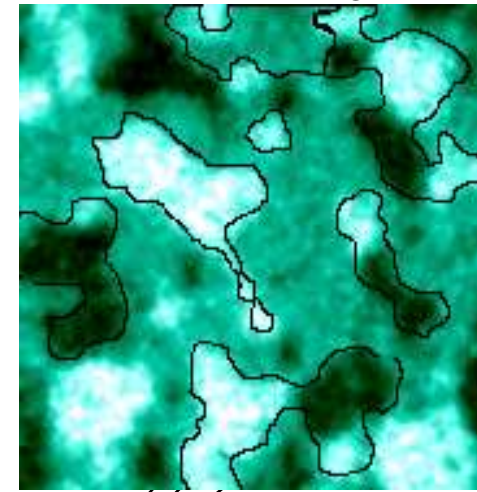
Photon Energy (eV)

Photon Energy (eV)

Adding the time domain to PEEM

TR-PEEM methods

Time-resolved PEEM: the stroboscopic approach

Stroboscopic experiments combine high lateral resolution of PEEM with high time resolution, taking advantage of pulsed nature of synchrotron radiation
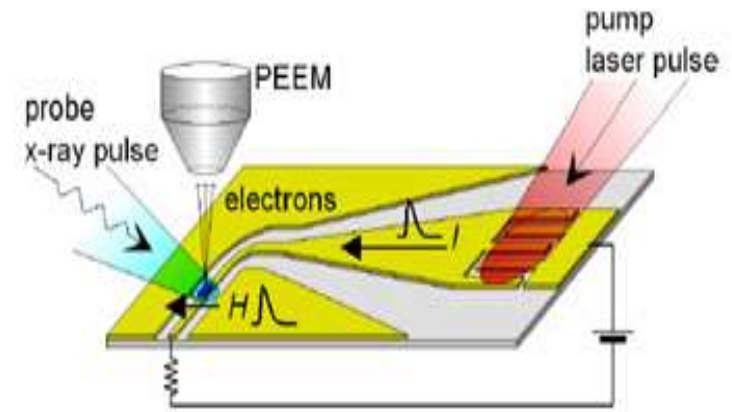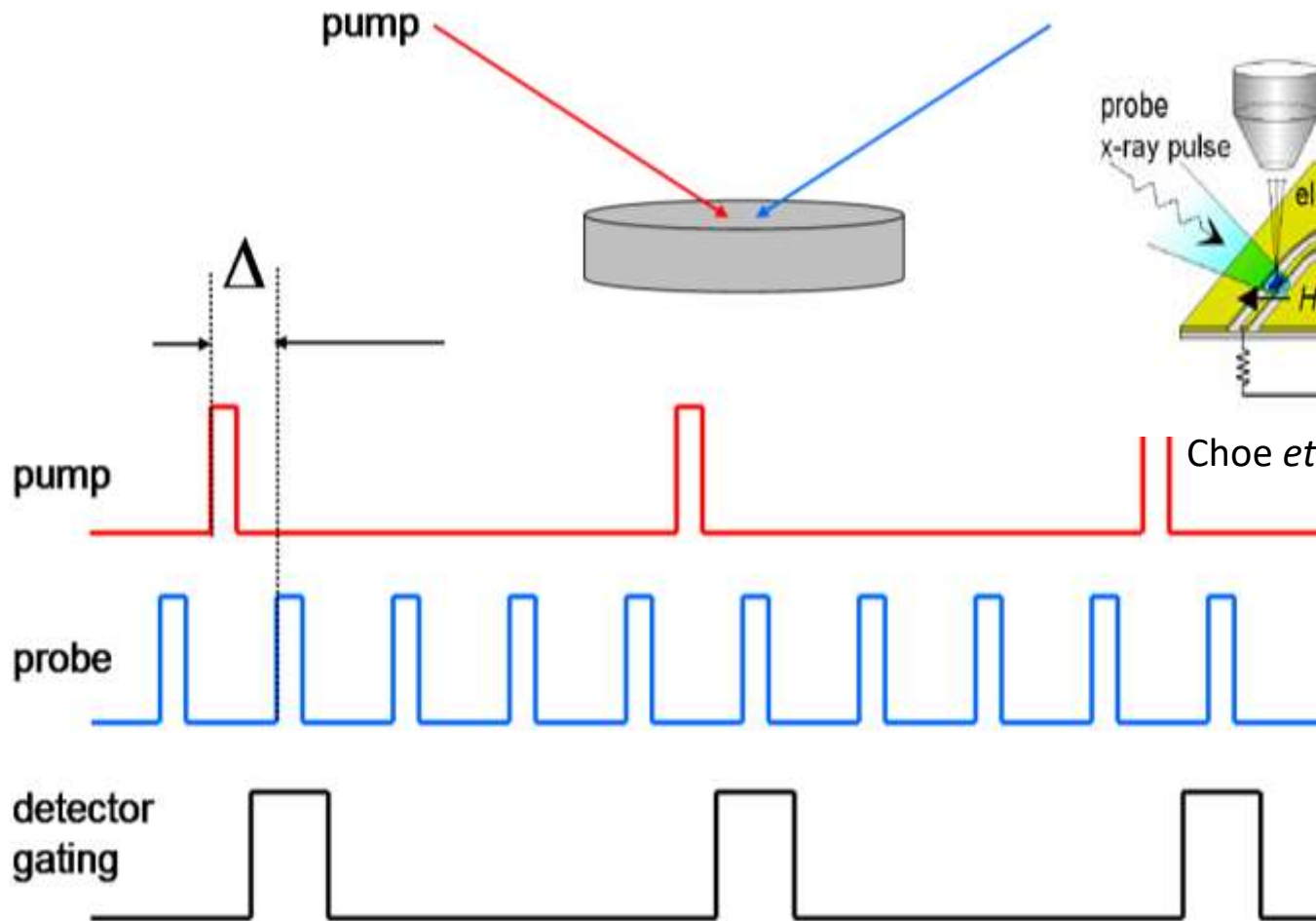
Choe *et al.,* Science 304, 420 (2004)

Time resolved XMCD-PEEM: applications

- **Switching processes** (magnetisation reversal) in magnetic elements (in spin valves, tunnel junction)
  - Nucleation, DW propagation or both
  - Effect of surface topography, morphology crystalline structure etc.
  - Domain dynamics in Landau flux closure structures.
- response of vortices, domains, domain walls in Landau closure domains in the **precessional regime**
- **Stroboscopic technique**:
  - only reversible processes can be studied by pump – probe experiments
  - Measurements are quantitative

Elettra Sincrotrone Trieste

Quantitative Analysis of Magnetic Excitations in Landau Flux-Closure Structures Using Synchrotron-Radiation Microscopy

J. Raabe,[1,*] C. Quitmann,[1] C. H. Back,[2] F. Nolting,[1] S. Johnson,[1] and C. Buehler[1]

The time dependent magnetization is described by the phenomenological Landau-Lifshitz-Gilbert equation

$$\frac{d}{dt}\vec{M} = -\gamma_0\vec{M} \times \vec{H}_{\text{eff}} + \frac{\alpha}{M}\left(\vec{M} \times \frac{d}{dt}\vec{M}\right).$$

The first term describes the precession of the magnetization $\vec{M}$ about the total effective field $\vec{H}_{\text{eff}}$. The second term describes the relaxation back into the equilibrium state using the dimensionless damping parameter α.

torque $\vec{T} = -\gamma_0\vec{M} \times \dot{\vec{H}}_{\text{eff}}$

xmcd

t_i-t

0

Summary
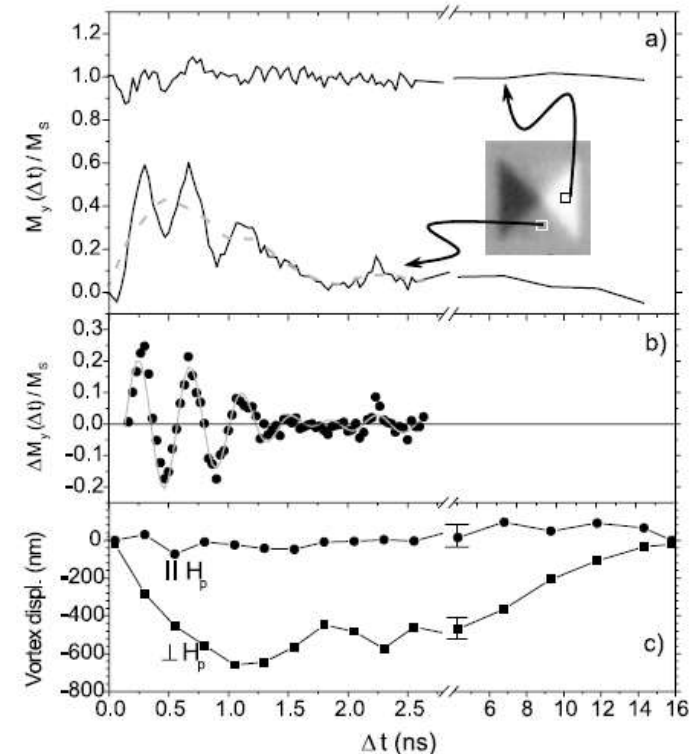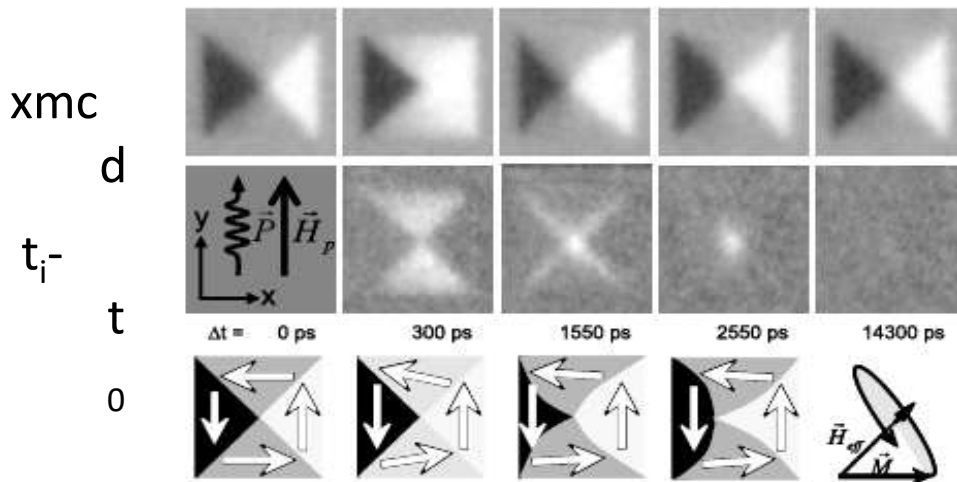
- XPEEM is a versatile full-field imaging technique. Combined with SR it allows us to implement laterally resolved versions of the most popular x-ray spectroscopies taking advantage of high flux of 3rd generation SR light sources.

- In particular, XAS-PEEM combines element sensitivity with chemical sensitivity (e.g. valence), and, more importantly, magnetic sensitivity. Magnetic imaging has been the most successful application of PEEM.

- XPEEM or energy-filtered PEEM adds true chemical sensitivity to PEEM. Modern instruments allow to combine chemical imaging with electronic structure imaging using ARUPS.

- XPEEM can be complemented by LEEM, which adds structure sensitivity and capability to monitor dynamic processes.

- Lateral resolution will approach the nm range as AC instruments become available. Limitations due to space charge are not yet clear

- Novel application field are being approached, such as biology, geology and earth sciences. HAXPES will increase our capabilities to probe buried structures (bulk).

Reviews on x-ray spectromicroscopy and XPEEM

- Bauer, E. Surface Microscopy with Low Energy Electrons; Springer: New York, 2014;
- Cheng, X. M.; Keavney, D. J. Studies of Nanomagnetism Using Synchrotron-based Xray Photoemission Electron Microscopy (X-PEEM). Rep. Prog. Phys. 2012, 75, 026501.
- E. Bauer, *Ultramicroscopy* **119**, 18–23 (2012).
- E. Bauer, *J. Electron. Spectrosc. Relat. Phenom*. (2012): http://dx.doi.org/10.1016/j.elspec.2012.08.001
- G. Margaritondo, *J. Electron. Spectrosc. Relat. Phenom.* **178–179**, 273–291 (2010) .
- A. Locatelli, E. Bauer, *J. Phys.: Condens. Matter* **20**, 093002 (2008) .
- G. Schönhense *et al*., in "*Adv. Imaging Electron Phys.*", vol. **142**, Elsevier, Amsterdam, P. Hawkes (Ed.), 2006, pp. 159–323.
- S. Guenther, B. Kaulich, L.Gregoratti, M. Kiskinova, *Prog. Surf. Sci.* **70**, 187–260 (2002).
- C.M. Schneider, G. Schönhense, *Rep. Prog. Phys.* **65**, R1785–R1839 (2002) .
- W. Kuch, in "*Magnetism: A Synchrotron Radiation Approach*", Springer, Berlin, E. Beaurepaire et al. (Eds.), 2006, pp. 275–320.
- J. Feng, A. Scholl, in P.W. Hawkes, "*Science of Microscopy*", Springer, New York, J.C.H. Spence (Eds.), 2007, pp. 657–695.
- E. Bauer and Th. Schmidt, in "*High Resolution Imaging and Spectroscopy of Materials*", Springer, Berlin, Heidelberg, F. Ernst and M. Ruehle (Eds.), 2002, pp. 363-390.
- E. Bauer, *J. Electron Spectrosc. Relat. Phenom.* **114-116,** 976-987 (2002).
- E. Bauer, *J. Phys.: Condens. Matter* **13,** 11391-11405 (2001).